



NOVA

University of Newcastle Research Online

nova.newcastle.edu.au

Weng, Zhe (Han); Van Zwieten, Lukas; Cozzolino, Daniel; Araujo, Joyce R.; Archanjo, Braulio S.; Cowie, Annette; Singh, Bhupinder Pal; Tavakkoli, Ehsan; Joseph, Stephen; Macdonald, Lynne M.; Rose, Terry J.; Rose, Michael T.; Kimber, Stephen W. L.; Morris, Stephen; ' Biochar built soil carbon over a decade by stabilizing rhizodeposits'.
Published in Nature Climate Change Vol. 7, Issue 5, p. 371-376 (2017)

Accessed from: <http://dx.doi.org/10.1038/NCLIMATE3276>

Accessed from: <http://hdl.handle.net/1959.13/1399682>

1 **Biochar built soil carbon over a decade by stabilising**
2 **rhizodeposits**

3 Zhe (Han) Weng^{1,2}, **Lukas Van Zwieten**^{1,3,4★}, Bhupinder Pal Singh^{1,5}, Ehsan Tavakkoli^{2,6},
4 Stephen Joseph^{7,8,9}, Lynne M. Macdonald¹⁰, Terry J. Rose⁴, Michael T. Rose³,
5 Stephen W. L. Kimber³, Stephen Morris³, Daniel Cozzolino¹¹, Joyce R. Araujo¹², Bráulio S
6 Archanjo¹² and Annette Cowie^{1,13}

7 1 School of Environmental and Rural Sciences, University of New England, Armidale, NSW 2351

8 2 Graham Centre for Agricultural Innovation, Charles Sturt University, Wagga Wagga, NSW 2650

9 3 NSW Department of Primary Industries, Wollongbar Primary Industries Institute, Wollongbar, NSW 2477

10 4 Southern Cross University, East Lismore, NSW 2480

11 5 NSW Department of Primary Industries, Elizabeth Macarthur Agricultural Institute, Woodbridge Rd, Menangle, NSW 2568

12 6 NSW Department of Primary Industries, Wagga Wagga Agricultural Institute, Wagga Wagga NSW 2650

13 7 University of Newcastle, Callaghan, NSW 2308

14 8 University of New South Wales, Sydney, NSW 2052

15 9 University of Wollongong, Wollongong, NSW 2522

16 10 CSIRO Agriculture, Waite campus, Glen Osmond, SA 5064

17 11 Central Queensland Innovation and Research Precinct, North Rockhampton, Central Queensland University, QLD 4701

18 12 Divisão de Metrologia de Materiais - DIMAT, Instituto Nacional de Metrologia, Normalização e Qualidade Industrial -

19 INMETRO, Duque de Caxias, RJ, 25250-020, Brazil

20 13 NSW Department of Primary Industries, Armidale, NSW 2351

21 ★Email: lukas.van.zwieten@dpi.nsw.gov.au

22 Biochar can increase the stable C content of soil. However, studies on the longer-term role of plant-soil-
23 biochar interactions and the consequential changes to native soil organic carbon (SOC) are lacking. Periodic
24 ^{13}C pulse-labelling of ryegrass was used to monitor belowground C allocation, SOC priming, and
25 stabilisation of root-derived C for a 15 month period – commencing 8.2 years after biochar (*Eucalyptus*
26 *saligna*, 550°C) was amended into a subtropical Ferralsol. We found that field-aged biochar amended soil
27 enhanced the belowground recovery of new root-derived C (^{13}C) by 20%, and facilitated negative
28 rhizosphere priming (slowed SOC mineralisation by 5.5%, *i.e.* 46 g $\text{CO}_2\text{-C m}^{-2} \text{y}^{-1}$). Retention of root-derived
29 ^{13}C in the stable organo-mineral fraction (<53 μm) was also increased (6%, $P < 0.05$). Through synchrotron-
30 based spectroscopic analysis of bulk soil, field-aged biochar and microaggregates (<250 μm), we
31 demonstrate that biochar accelerates the formation of microaggregates via organo-mineral interactions,
32 resulting in the stabilisation and accumulation of SOC in a rhodic Ferralsol.

33 Soil organic carbon (SOC) plays a vital role in maintaining soil quality and ecosystem functions, supporting
34 agronomic productivity and resilience of agro-ecosystems to mitigate climate change¹. While soils contain an
35 estimated $1.5 \times 10^3 \text{ Pg C}$ to 1 m depth² – accounting for almost 50% of the terrestrial C pool – human activities
36 and land use changes have reduced SOC in agricultural lands by $0.5\text{-}2 \text{ Mg C ha}^{-1} \text{ yr}^{-1}$ (ref.3). Potential exists to
37 restore or increase SOC levels ($0.1\text{-}1.0 \text{ Mg C ha}^{-1} \text{ yr}^{-1}$ globally²) to sustain the productivity of agro-ecosystems
38 and sequester C to mitigate climate change. However, a better understanding is needed of the processes
39 involved in controlling SOC fluxes (*i.e.* inputs and outputs) under various soil C management practices. Of
40 particular relevance are tropical soils, which currently represent 11–13% of the total global soil C reserve.
41 Covering vast tropical and subtropical areas (~0.75 Gha), Ferralsols (Fe-dominant soils) have been identified as
42 being particularly vulnerable to degradation and erosion over the next 50 years⁴. We propose that biochar
43 amendment of Ferralsols is an important strategy to enhance soil C stocks and productivity.

44 Biochar is defined as a solid material produced from thermochemical conversion of biomass under oxygen (O_2)
45 limitation, used as a soil amendment and for environmental applications in which C is retained. It is estimated
46 to have a negative emission potential of $0.7 \text{ Pg C eq. yr}^{-1}$ (ref.5,6), based on (a) reduced biomass decay due to
47 stabilisation of organic matter^{7,8}, and (b) indirect net effects including lowered CH_4 and N_2O emissions⁹, and
48 enhanced productivity^{10,11}. Further, biochar may facilitate negative priming in soil¹²⁻¹⁴ due to the decreased
49 rate of turnover of both existing soil organic matter (SOM) and newly-added root-derived C compounds.

50 However, the results of studies on the longevity and magnitude of priming effects, ranging from weeks to
51 several years, vary widely due to the heterogeneity of biochar-amended soil systems¹⁵. While some studies
52 found that biochar-induced priming gave up to 5-fold losses of native SOC¹⁶, others studies showed negligible
53 positive priming¹⁷. More recent studies incorporating plants in experimental systems have found substantial
54 negative priming, which lowered cumulative SOC mineralisation by 16-48% compared to controls in
55 laboratory¹², glasshouse¹⁴ and field¹³ settings. While the mechanisms responsible for biochar-induced priming
56 of SOC in planted systems are not yet resolved, physical protection of SOC is proposed as the most important
57 mechanism¹⁵.

58 The role of macroaggregate-occluded microaggregates (53-250 μm) in the long-term physical protection of
59 SOC has been demonstrated across widely varying agroecosystems, soil types and environments^{18,19}. A key
60 control of protective SOC stabilisation is the formation of mineral-organic associations (MOAs), which can
61 account for up to 91% of the total soil C²⁰. In humid environments the capacity of the mineral matrix to protect
62 SOM against mineralisation is largely controlled by the content of poorly crystalline minerals^{21,22}. In
63 (sub)tropical soils, SOM is mainly stabilised through complexation with Fe and Al oxyhydroxides and
64 interaction with clay particles²³. It has been proposed that biochar additions to soil may enhance these organo-
65 mineral interactions²⁴ via adsorption and/or ligand exchange reactions²⁵, which may further stabilise SOC. In
66 contrast, exudation of organic acids by plant roots has been found to accelerate the turnover and
67 transformation of MOAs²⁰. This process can lead to the loss of SOC stabilised in MOAs via simultaneous
68 degradation of both rhizodeposits (new root-derived C) and mineral-protected C²⁶ (native SOC and aged root-
69 derived C; Fig. 1a). The input of root exudates has also been reported to mediate SOC turnover in
70 unamended²⁷ and biochar-amended soils^{14,28}. The mechanisms of belowground C retention or loss within
71 systems where plant-derived C interacts with biochar and soil, particularly across a decadal time scale, remain
72 unknown²⁹.

73 Here we investigate the magnitude of rhizosphere SOC priming nearly a decade following the incorporation of
74 biochar into soil, by superimposing a 15-month repeated ¹³C pulse labelling experiment on a field study
75 established 8.2 years previously on a rhodic Ferralsol³⁰. In this subtropical annual ryegrass field system,
76 managed to supply year round high quality feed for dairy production, Slavich et al.³⁰ found an increase of 13.3 t
77 C ha⁻¹ in the total SOC stock (0-100 mm soil depth) at 36 months after the incorporation of biochar (*Eucalyptus*

78 *saligna*, 550°C). This SOC stock was nearly double that of the biochar-C addition alone (7.6 t C ha⁻¹ based on a
79 dose of 10 t biochar ha⁻¹, with 76% C content). Our study shows negative rhizosphere SOC priming in the aged
80 biochar-amended soil, and highlights several potential biochar-mediated mechanisms for enhanced
81 stabilisation of rhizodeposits in organo-mineral fractions (Fig. 1b), including: a) lowering microbial
82 mineralisation of native SOC (*cf.* control), and b) counteracting root-exudate-driven dissolution of mineral-
83 protected SOC²⁶ via enhanced organo-mineral interactions. We propose a mechanism for the accelerated
84 formation of organo-mineral microstructures (<53 µm) that accumulated plant-derived C in the 9.5-year field-
85 aged biochar-amended soil. We demonstrate that over a decade, biochar has a C sequestration potential well
86 in excess of the recalcitrant C in the biochar, in this Ferralsol.

87 **Negative priming of native SOC**

88 The use of specialised respiration collars to isolate soil + root respiration from shoot respiration¹³, combined
89 with periodic ¹³CO₂ pulse labelling over 15 months (between 8.2 and 9.5 years post biochar addition) allowed
90 us to quantify *in-situ* the rhizosphere priming of native SOC in the pasture site described above⁹. We used the
91 ¹³C end-member of biochar plus root (¹³C_{B+R}) to partition and quantify native SOC mineralisation (C_S) from the
92 combined 'plant-biochar' and native SOC sources:

$$93 \quad C_S(\%) = 100 * (\delta^{13}C_T - \delta^{13}C_{B+R}) / (\delta^{13}C_S - \delta^{13}C_{B+R})$$

94 where $\delta^{13}C_T$ is the $\delta^{13}C$ signature of the total CO₂-C evolved from the planted biochar-amended soil after pulse
95 labelling; $\delta^{13}C_{B+R}$ is the $\delta^{13}C$ signature of biochar plus root (obtained from a sand collar) after pulse labelling;
96 $\delta^{13}C_S$ is the $\delta^{13}C$ signature of the soil-derived CO₂-C evolved from the unplanted and unamended soil, which
97 was not pulse labelled. To minimise C isotopic fractionation during photosynthesis due to water stress³¹, the
98 biochar plus root sand collars and biochar plus soil plus root collars were regularly watered to similar moisture
99 content (60-80% water holding capacity).

100 We incubated fresh and extracted field-aged biochar in the dark over 16 hours in the laboratory (20°C) and
101 determined the $\delta^{13}C$ signature of the biochar-derived CO₂. We found no difference between the $\delta^{13}C$
102 signatures of fresh (the same biochar archived in a sealed container for 9.5 years) (-25.02 ± 0.13‰) and field-
103 aged biochar (-25.04 ± 0.11‰), thus validating the use of archived biochar in the sand collar. Furthermore, the

104 aged-biochar ^{13}C (C_3 -dominated) would vary in a narrow range during its mineralisation relative to soil ^{13}C from
105 a mixture of C_3 and C_4 pools. Additionally, the level of $\delta^{13}\text{C}$ enrichment of the root component was much
106 greater than any isotopic signature contribution from soil and biochar to the $\delta^{13}\text{C}_T$ (online method section),
107 hence surpassing any interactive effect of biochar and plant on the $\delta^{13}\text{C}_S$ (Fig. 2b). Three scenarios were used
108 to interpret the results with respect to SOC source partitioning in the planted biochar systems: 1) extreme
109 positive priming of recent SOC derived from the current ryegrass (C_3) pasture; 2) no rhizosphere priming of
110 SOC; and 3) extreme positive priming of the native C_4 -dominant SOC. Details of the sensitivity analysis can be
111 found in the online method section.

112 The cumulative SOC mineralisation between 8.2 and 9.5 years was calculated as the area of a linear
113 interpolation across all measurement points in the biochar-amended and unamended systems. Rhizosphere
114 SOC priming was calculated as the difference between cumulative SOC mineralisation in the planted soil and
115 the unplanted soil in the unamended system (Fig. 2a and Fig. S5a, online method section) and the biochar-
116 amended system (Fig. 2b and Fig. S5b), respectively. The biochar amendment induced significant negative
117 rhizosphere SOC priming 9.5 years after being incorporated into the planted Ferralsol (Fig. 2b). As a result, SOC
118 mineralisation was lowered by $46.1 (\pm 19.5) \text{ g CO}_2\text{-C m}^{-2}$ between 8.2 and 9.5 years in the planted biochar-
119 amended soil compared to the unplanted biochar-amended soil ($P < 0.05$), thus contributing to the measured
120 (ca. 10%) increase in the total SOC stock (Fig. 3a, $P < 0.05$). In the absence of biochar, root activity triggered
121 significant positive priming of SOC, increasing SOC mineralisation by $60.7 (\pm 21.1) \text{ g CO}_2\text{-C m}^{-2}$ between 8.2 and
122 9.5 years compared to the unplanted unamended soil (Fig. 2a).

123 To determine the contribution of microbial processes to the negative rhizosphere priming of SOC in the
124 presence of biochar, we measured a) metabolic quotients associated with native SOC (*i.e.* bulk) and
125 rhizodeposition (*i.e.* new C labelled with ^{13}C), and b) catabolic enzyme activities. The bulk metabolic quotient in
126 the biochar-amended soil ($0.158 \pm 0.053 \mu\text{g CO}_2\text{-C mg}^{-1} \text{ microbial biomass carbon (MBC) h}^{-1}$) was significantly
127 lower ($P < 0.05$) than that of the control soil ($0.287 \pm 0.022 \mu\text{g CO}_2\text{-C mg}^{-1} \text{ MBC h}^{-1}$), despite no difference
128 between the metabolic quotient associated with new C (Table S1), catabolic enzyme activities (B-glucosidase,
129 xylosidase, cellulase, N-acetyl-glucosaminidase, Table S2) or substrate-induced respiration using 15 different C
130 substrates (Microresp™, Fig. S1). These results confirm that biochar amendment is likely to have improved the
131 efficiency of native SOC use by soil microorganisms, as previously reported^{32,33}.

132 **Belowground C stabilisation**

133 The contribution of microbial processes to negative SOC priming may be only transient²⁴. To provide a
134 mechanistic understanding of the persistent negative rhizosphere priming of SOC in the presence of biochar,
135 we performed a detailed soil physical fractionation coupled with stable ¹³C isotope and spectroscopic analyses
136 to quantify the magnitude and fate of newly fixed ¹³C within the various belowground C pools. Belowground
137 ¹³C recovery was greater in the biochar-amended soil at 9.5-years after amendment than that of the control,
138 largely due to a lowering (2%) of soil + root respiration, and an increase in ¹³C associated with root biomass
139 (8%; P<0.05), occluded-particulate organic matter (o-POM, 4%; P<0.05), and mineral-protected SOM (m-SOM,
140 6%; P<0.05, Fig. 1). Despite the lack of effect of biochar on the measured root biomass C at harvest (9.5 years,
141 Fig. 3b), it has been reported that biochar increased C and nutrient retention³⁴ via organo-mineral
142 interactions¹⁶ upon ageing in soil. Hence, biochar may retain more C from root exudates. Greater belowground
143 recovery of the new root-derived ¹³C in the biochar-amended soil suggests that biochar may have increased
144 root activity (exudation) and contributed to the soil aggregation process, followed by enhanced protection of
145 root-derived POM-C or exudates through physical occlusion or upon interaction with minerals²⁵.

146 The total recovered ¹³C (*i.e.* soil + root respiration, root, free POM, o-POM and m-SOM) was also greater (P<
147 0.05) in the biochar-amended soil (60.7 ± 9.9%) than the control (42.2 ± 3.8%) at the 3rd pulse labelling event
148 (Year 9.5, Fig. S2). Root biomass ¹³C decreased by 19% and 11% between the 1st (Year 8.9) and 3rd (Year 9.5)
149 labelling events in the control and biochar-amended soils, respectively. Meanwhile, o-POM increased by 10%
150 and 7% and m-SOM by 24% and 27% in the control and biochar-amended soils, respectively (P< 0.05, Fig. S2).
151 These results complement the study of Desjardins et al.³⁵, where the rapid entrapment of young OM was
152 observed in the finest fractions (*i.e.* clay-sized microaggregates) in an Amazonian pasture soil.

153 **Spectroscopic insights into priming**

154 To further develop the mechanistic understanding of stabilisation processes, we used synchrotron-based soft
155 x-ray (SXR) analysis of the bulk soils (control and biochar-amended soils under the ryegrass pasture). We
156 support this with SXR analysis of field extracted 9.5-year aged biochar and its corresponding archived biochar.
157 The C functional groups from the biochar-amended soil feature prominent resonances assigned to quinones
158 (284.1 eV), aromatic C (285.2 eV, 1s-π* transitions of conjugated C=C), and aliphatic C (287.3 eV) in the SXR

159 spectra (Fig. 4a). At higher energies, greater carboxyl C–OOH (288.6 eV) and C–O (289.3eV) intensities of
160 (hemi)cellulose and lignin³⁶, respectively, were found in the aged biochar-amended soil *cf.* the control. The
161 greater intensities of these peaks can be largely explained by the biochar feedstock material (*Eucalyptus*
162 *saligna*). (Hemi)Cellulose and lignin would be largely absent from native SOM in this Ferralsol, which has been
163 under managed pasture for *ca.* 100 years. The notable peak at 287.3 eV (corresponding to aliphatic C–H and
164 phenolic C–OH³⁶), only apparent in the planted biochar-amended soil, suggests the preferential stabilisation of
165 lipophilic plant-derived C in the presence of biochar. This is supported by the negative rhizosphere priming of
166 SOC observed between 8.2 and 9.5 years after biochar incorporation (Fig. 2b). Furthermore, biochar has been
167 shown to contain quinones^{37,38}, potentially explaining the more distinct resonance associated with quinones in
168 the biochar-amended soil *cf.* the unamended control soil.

169 We further investigated the changes in the composition of SOM by analysing the same samples with Fourier
170 Transform Infrared Spectroscopy (FTIR; Fig. 4b). The average FTIR spectra for the biochar-amended and control
171 soils are similar, but a number of distinct characteristics were identified in the frequency range of 4000 to 600
172 cm^{-1} for major absorbance peaks in the biochar-amended soil representing new root-derived C, native SOC³⁹
173 and biochar-C⁴⁰. The broad intense band at about 3530 cm^{-1} indicates mainly O–H stretching of carboxylic
174 acids, phenols and alcohols. The greater N–H contribution (*i.e.* O–H, N–H stretching of amines) is represented
175 at 3450 cm^{-1} . The broad band at 1100 cm^{-1} was assigned primarily to ester, phenol C–O–C and C–OH
176 stretching, which could be attributed to polysaccharides or polysaccharide-like compounds. The strong band
177 at 828 cm^{-1} represents out-of-plane aromatic C–H bending vibrations⁴¹. When the mean second derivative
178 spectra were compared (Fig. 4c), the longer-term impact of biochar on SOM was further highlighted by the
179 aromatic groups (quinones, 1750 cm^{-1}), CN triple bonds (2355 cm^{-1}), and carboxyl groups (C–C, 1500–1650 cm^{-1}),
180 as well as C–H and C–C groups (1400 cm^{-1}). The representative peaks for aromatic C were better resolved in
181 the second derivative spectra, including C–H stretching (750–900 and 3050–3000 cm^{-1}), C = C (1380–1450
182 cm^{-1}), C–C, and C–O stretching (1580–1700 cm^{-1}). These findings support the identification of aliphatic C
183 groups and (hemi)cellulose in the biochar-amended soil by SXR. Crosslinking of organic matter through
184 functional groups such as carboxyl and phenolic moieties with multivalent cations has been suggested to
185 facilitate organo–mineral interactions⁴². Thus these spectroscopic data support the interpretation that biochar
186 facilitates the stabilisation of organic compounds through organo–mineral interactions²⁵.

187 The finely crushed microaggregate fraction (<250 μm , Table S10) was analysed by X-ray photoelectron
188 spectroscopy (XPS), showing a higher concentration of C=O and COOH functional groups in the biochar–
189 amended soil *cf.* the control soil. In this fraction, the C–1s photoelectron peak was composed of four
190 components (Table S10): C1s A in 284.6 eV from aromatic C (C=C); C1s B in 286.2 ± 0.2 eV, which may be
191 assigned to phenol or hydroxyl (C–OH) groups, ether (C–O–C) or pyrrolic (C–N) groups; C–1s C in 287.5 ± 0.4
192 eV, assigned to carbonyl (C=O) groups; and C–1s D in 289.1 ± 0.3 eV, assigned to the carboxyl (COOH) groups⁴³,
193 ⁴⁴. Increase in carboxyl groups over time in biochar–amended soils has been shown on numerous occasions,
194 from month–long incubation trials ⁴⁵ to centennial⁴⁶ and millennial time scales⁴⁷. This oxidation can be a result
195 of the adsorption of dissolved organic C (*e.g.* root exudates) by biochar⁴⁸, which may explain the observed
196 negative priming in the planted biochar–amended soil between 8.2 and 9.5 years post-amendment (Fig. 2b) *cf.*
197 the positive priming in the planted unamended soil (Fig. 2a).

198 **Global impact of stabilising rhizodeposits**

199 The long–term stabilisation of rhizodeposits by biochar amendment has significant implications for increasing
200 SOC sequestration potential beyond the recalcitrant C contained in the biochar. Pasture systems may allocate
201 nearly 40% of their fixed C to the belowground compartment as rhizodeposits⁴⁹ (*i.e.* exudates, soluble lysates,
202 mucilage, sloughed–off root cells and tissues). Hence, the retention of belowground C inputs by the
203 application of biochar¹² could play a major role in C sequestration in grasslands⁵⁰, which occupy an area of 3.5
204 Gha worldwide². Studies assessing impacts of climate change on soil C consistently indicate that a warmer
205 climate will lower C stocks in tropical soils⁵¹. Ferralsols, an important soil type in the (sub)tropical regions, are
206 particularly sensitive to degradation and erosion under future climate change⁴. The increased stabilisation of
207 rhizodeposits observed in this study could represent a significant global C sequestration potential across
208 (sub)tropical Ferralsol pastures⁵².

209 We showed that SOC stabilisation in o-POM and m-SOM fractions (*i.e.* retention of new C in ‘O’ and ‘M’ pools
210 over the initial ¹³C labelled amount in Fig. 1) was increased by 10% in the biochar-amended soil *cf.* the control.
211 To demonstrate the possible magnitude of increased SOC sequestration, we extrapolated this 10% increase in
212 stabilisation based on the potential for woody biochar production⁵³ (online method section). We estimate the
213 additional biochar–induced SOC sequestration to be in the range of 0.03–0.04 Pg C y^{-1} globally. This additional

214 sequestration mechanism would increase the mitigation potential of biochar (*i.e.* 130 Pg C over a century⁶) by
215 2.3–3.1%. Further research is required to validate these outcomes and proposed mechanisms of plant-derived
216 C stabilisation in other agroecosystems, noting that lower priming and stabilisation is likely in cropping systems
217 due to lower belowground C allocation⁵² and that the effect may vary further depending on soil texture and
218 clay mineralogy⁵⁴.

219 Using our long-term biochar experimental field site, we found that biochar addition to a subtropical Ferralsol
220 pasture built soil C by forming organo–mineral microstructures (<53 μm) that enhanced the retention of root-
221 derived C by 20%. Negative priming as a result of biochar amendment was detected at nearly a decade after its
222 incorporation. We showed that biochar slowed SOC mineralisation by 5.5 % (*i.e.* 46 g CO₂-C m⁻² y⁻¹). Based on
223 SRX and FTIR analyses, we suggest that the sorption of root exudates on biochar surfaces may counteract the
224 dissolution of mineral–protected SOC catalysed by root exudates.

225 References

- 226 1 Lal, R. Managing soils and ecosystems for mitigating anthropogenic carbon emissions and advancing global food
227 security. *BioScience* **60**, 708–721 (2010).
- 228 2 Antle, J. M., Capalbo, S. M., Mooney, S., Elliott, E. T., & Paustian, K. H. Economic analysis of agricultural soil
229 carbon sequestration: an integrated assessment approach. *Journal of agricultural and resource economics* **26**,
230 344–367 (2001).
- 231 3 Ogle, S. M., Breidt, F. J. & Paustian, K. Agricultural management impacts on soil organic carbon storage under
232 moist and dry climatic conditions of temperate and tropical regions. *Biogeochemistry* **72**, 87–121 (2005).
- 233 4 Stocking, M. A. Tropical soils and food security: the next 50 years. *Science* **302**, 1356–1359 (2003).
- 234 5 Smith, P. Soil carbon sequestration and biochar as negative emission technologies. *Global Change Biology* **22**,
235 1315–1324 (2016).
- 236 6 Woolf, D., Amonette, J. E., Street–Perrott, F. A., Lehmann, J. & Joseph, S. Sustainable biochar to mitigate global
237 climate change. *Nature Communications* **1**, 56 (2010).
- 238 7 Singh, B. P. & Cowie, A. L. Long–term influence of biochar on native organic carbon mineralisation in a low–
239 carbon clayey soil. *Scientific Reports* **4** (2014).
- 240 8 Zimmerman, A. R. & Gao, B. The stability of biochar in the environment. *Biochar and Soil Biota*, 1 (2013).
- 241 9 Van Zwieten L, Kammann C, Cayuela M, Singh BP, Joseph S, Kimber S, Clough T, & Spokas K. Biochar effects on
242 nitrous oxide and methane emissions from soil. *Biochar for Environmental Management: Science, Technology and
243 Implementation (second edition)*. New York: Routledge, 489–520 (2015).
- 244 10 Novak, J. M. *et al.* Short–term CO₂ mineralization after additions of biochar and switchgrass to a Typic
245 Kandiudult. *Geoderma* **154**, 281–288 (2010).
- 246 11 Van Zwieten, L. *et al.* Effects of biochar from slow pyrolysis of papermill waste on agronomic performance and
247 soil fertility. *Plant and Soil* **327**, 235–246 (2010).
- 248 12 Keith, A., Singh, B. & Dijkstra, F. A. Biochar reduces the rhizosphere priming effect on soil organic carbon. *Soil
249 Biology and Biochemistry* **88**, 372–379 (2015).
- 250 13 Weng, Z. *et al.* Plant–biochar interactions drive the negative priming of soil organic carbon in an annual ryegrass
251 field system. *Soil Biology and Biochemistry* **90**, 111–121 (2015).
- 252 14 Whitman, T., Enders, A. & Lehmann, J. Pyrogenic carbon additions to soil counteract positive priming of soil
253 carbon mineralization by plants. *Soil Biology & Biochemistry* **73**, 33–41 (2014).
- 254 15 Maestrini, B., Nannipieri, P. & Abiven, S. A meta–analysis on pyrogenic organic matter induced priming effect.
255 *GCB Bioenergy* **7(4)**, 577–590 (2014).
- 256 16 Luo, Y., Durenkamp, M., De Nobili, M., Lin, Q. & Brookes, P. C. Short term soil priming effects and the
257 mineralisation of biochar following its incorporation to soils of different pH. *Soil Biology & Biochemistry* **43**,
258 2304–2314 (2011).
- 259 17 Kuzuyakov, Y., Subbotina, I., Chen, H., Bogomolova, I. & Xu, X. Black carbon decomposition and incorporation into
260 soil microbial biomass estimated by C–14 labeling. *Soil Biology & Biochemistry* **41**, 210–219 (2009).

- 261 18 Six, J., Elliott, E. T., Paustian, K. & Doran, J. W. Aggregation and soil organic matter accumulation in cultivated and
262 native grassland soils. *Soil Science Society of America Journal* **62**, 1367–1377 (1998).
- 263 19 Kong, A. Y., Six, J., Bryant, D. C., Denison, R. F. & Van Kessel, C. The relationship between carbon input,
264 aggregation, and soil organic carbon stabilization in sustainable cropping systems. *Soil Science Society of America
265 Journal* **69**, 1078–1085 (2005).
- 266 20 Kleber M, Eusterhues K, Keiluweit M, Mikutta C, Mikutta R, Nico PS. Chapter One—Mineral—Organic Associations:
267 Formation, Properties, and Relevance in Soil Environments. *Advances in Agronomy* **130**, 1–40 (2015).
- 268 21 Torn, M. S., Trumbore, S. E., Chadwick, O. A., Vitousek, P. M. & Hendricks, D. M. Mineral control of soil organic
269 carbon storage and turnover. *Nature* **389**, 170–173 (1997).
- 270 22 Mikutta, R., Kleber, M. & Jahn, R. Poorly crystalline minerals protect organic carbon in clay subfractions from acid
271 subsoil horizons. *Geoderma* **128**, 106–115 (2005).
- 272 23 Denef, K., Plante, A. & Six, J. Characterization of soil organic matter. *Soil Carbon Dynamics: An Integrated
273 Methodology*. Cambridge University Press, New York, 91–126 (2009).
- 274 24 Singh, B. P., Cowie, A. L. & Smernik, R. J. Biochar Carbon Stability in a Clayey Soil As a Function of Feedstock and
275 Pyrolysis Temperature. *Environmental Science & Technology* **46** (2012).
- 276 25 Joseph, S. D. *et al.* An investigation into the reactions of biochar in soil. *Australian Journal of Soil Research* **48**
277 (2010).
- 278 26 Keiluweit, M. *et al.* Mineral protection of soil carbon counteracted by root exudates. *Nature Climate Change* **5**,
279 588–595 (2015).
- 280 27 Haichar, F. e. Z., Santaella, C., Heulin, T. & Achouak, W. Root exudates mediated interactions belowground. *Soil
281 Biology and Biochemistry* **77**, 69–80 (2014).
- 282 28 Ventura, M. *et al.* Effect of biochar addition on soil respiration partitioning and root dynamics in an apple
283 orchard. *European Journal of Soil Science* **65**, 186–195 (2014).
- 284 29 Whitman, T., Singh, B. P. & Zimmerman, A. Priming effects in biochar-amended soils: implications of biochar–soil
285 organic matter interactions for carbon storage. *Biochar for Environmental Management: Science, Technology and
286 Implementation (second edition)*. New York: Routledge, **455–488** (2015).
- 287 30 Slavich, P. G. *et al.* Contrasting effects of manure and green waste biochars on the properties of an acidic ferralsol
288 and productivity of a subtropical pasture. *Plant and Soil* **366**, 213–227 (2013).
- 289 31 Farquhar, G. D., Ehleringer, J. R. & Hubick, K. T. Carbon isotope discrimination and photosynthesis. *Annual review
290 of plant biology* **40**, 503–537 (1989).
- 291 32 Lehmann, J. *et al.* Biochar effects on soil biota – A review. *Soil Biology & Biochemistry* **43**, 1812–1836 (2011).
- 292 33 Liang, B. *et al.* Black carbon affects the cycling of non-black carbon in soil. *Organic Geochemistry* **41**, 206–213
293 (2010).
- 294 34 Lawrinenko, M. & Laird, D. A. Anion exchange capacity of biochar. *Green Chemistry* **17**, 4628–4636 (2015).
- 295 35 Desjardins, T., Barros, E., Sarrazin, M., Girardin, C. & Mariotti, A. Effects of forest conversion to pasture on soil
296 carbon content and dynamics in Brazilian Amazonia. *Agriculture, Ecosystems & Environment* **103**, 365–373
297 (2004).
- 298 36 Solomon, D. *et al.* Micro- and nano-environments of carbon sequestration: Multi-element STXM–NEXAFS
299 spectromicroscopy assessment of microbial carbon and mineral associations. *Chemical Geology* **329**, 53–73
300 (2012).
- 301 37 Solomon, D. *et al.* Molecular signature and sources of biochemical recalcitrance of organic C in Amazonian Dark
302 Earths. *Geochimica et Cosmochimica Acta* **71**, 2285–2298 (2007).
- 303 38 Heymann, K., Lehmann, J., Solomon, D., Schmidt, M. W. & Regier, T. C 1s K-edge near edge X-ray absorption fine
304 structure (NEXAFS) spectroscopy for characterizing functional group chemistry of black carbon. *Organic
305 Geochemistry* **42**, 1055–1064 (2011).
- 306 39 Solomon, D., Lehmann, J., Kinyangi, J., Liang, B. & Schäfer, T. Carbon K-edge NEXAFS and FTIR–ATR spectroscopic
307 investigation of organic carbon speciation in soils. *Soil Science Society of America Journal* **69**, 107–119 (2005).
- 308 40 Rutherford, D. W., Wershaw, R. L., Rostad, C. E. & Kelly, C. N. Effect of formation conditions on biochars:
309 compositional and structural properties of cellulose, lignin, and pine biochars. *Biomass and Bioenergy* **46**, 693–
310 701 (2012).
- 311 41 Artz, R. R. *et al.* FTIR spectroscopy can be used as a screening tool for organic matter quality in regenerating
312 cutover peatlands. *Soil Biology and Biochemistry* **40**, 515–527 (2008).
- 313 42 Mouvenchery, Y. K., Kučerík, J., Diehl, D. & Schaumann, G. E. Cation-mediated cross-linking in natural organic
314 matter: a review. *Reviews in Environmental Science and Biotechnology* **11**, 41–54 (2012).
- 315 43 Archanjo, B. S. *et al.* Chemical analysis and molecular models for calcium–oxygen–carbon interactions in black
316 carbon found in fertile Amazonian anthrosoils. *Environmental Science & Technology* **48**, 7445–7452 (2014).
- 317 44 Araujo, J. R. *et al.* Selective extraction of humic acids from an anthropogenic Amazonian dark earth and from a
318 chemically oxidized charcoal. *Biology and Fertility of Soils* **50**, 1223–1232 (2014).
- 319 45 Cheng, C.–H., Lehmann, J., Thies, J. E., Burton, S. D. & Engelhard, M. H. Oxidation of black carbon by biotic and
320 abiotic processes. *Organic Geochemistry* **37**, 1477–1488 (2006).
- 321 46 Nguyen, B. T. *et al.* Long-term black carbon dynamics in cultivated soil. *Biogeochemistry* **89**, 295–308 (2008).

- 322 47 Lehmann, J. *et al.* Near-edge X-ray absorption fine structure (NEXAFS) spectroscopy for mapping nano-scale
323 distribution of organic carbon forms in soil: Application to black carbon particles. *Global Biogeochemical Cycles*
324 **19** (2005).
- 325 48 Pietikäinen, J., Kiikkilä, O. & Fritze, H. Charcoal as a habitat for microbes and its effect on the microbial
326 community of the underlying humus. *Oikos* **89**, 231–242 (2000).
- 327 49 Hafner, S. *et al.* Effect of grazing on carbon stocks and assimilate partitioning in a Tibetan montane pasture
328 revealed by ¹³C pulse labeling. *Global Change Biology* **18**, 528–538 (2012).
- 329 50 Singh, B. P. *et al.* In situ persistence and migration of biochar carbon and its impact on native carbon emission in
330 contrasting soils under managed temperate pastures. *PLoS One* **10** (2015).
- 331 51 Pachauri, R. K. *et al.* Climate Change 2014: Synthesis Report. Contribution of Working Groups I, II and III to the
332 Fifth Assessment Report of the Intergovernmental Panel on Climate Change. (2014).
- 333 52 Lal, R. Soil carbon sequestration to mitigate climate change. *Geoderma* **123**, 1–22 (2004).
- 334 53 Lehmann, J., Gaunt, J. & Rondon, M. Bio-char sequestration in terrestrial ecosystems—a review. *Mitigation and*
335 *adaptation strategies for global change* **11**, 395–419 (2006).
- 336 54 Fang, Y., Singh, B. & Singh, B. P. Effect of temperature on biochar priming effects and its stability in soils. *Soil*
337 *Biology & Biochemistry* **80**, 136–145 (2015).

338 **Statement of correspondence**

339 For further information, please contact Dr Lukas Van Zwieten via email: lukas.van.zwieten@dpi.nsw.gov.au

340 **Acknowledgement**

341 The authors thank the Australian Government, Department of Agriculture and Water Resources for supporting
342 the National Biochar Initiatives (2009–2012, 2012–2014) which co-funded this research. We are particularly
343 grateful to Dr. Peter Slavich, as one of the key founders of this long-term field experiment for providing
344 insightful comments on the initial draft. Part of this research was undertaken on the soft x-ray spectroscopy
345 beamline at the Australian Synchrotron, Victoria, Australia (grant number AS151_SXR_9599). We thank the
346 chief beamline scientist, Dr Bruce Cowie, for his technical support on the soft x ray analysis. We also
347 appreciate the technical support from Scott Petty and Josh Rust for maintaining this field experiment over the
348 past decade, and laboratory support from Nichole Morris. We also thank Dr Carlos Achete from INMETRO,
349 Brazil and Dr Bin Gong from the University of New South Wales, Australia, for performing XPS analysis of
350 biochars and soils, respectively. We acknowledge the intellectual contribution from Prof Scott Donne for
351 discussions on the potential mechanisms of biochar-induced stabilisation of rhizodeposits. We also thank Dr
352 Yunying Fang for giving advice and reviewing ¹³C calculations.

353 **Statement of author contribution**

354 ZW drafted and wrote the manuscript, experimental design, set-up and conducted experiments, and data
355 collection and analysis; LVZ and BPS wrote the manuscript, aided in experimental design, critical revision of the
356 article; ET aided in experimental design, data collection and analysis, critical revision of the article; SJ and MTR
357 collected and analysed data, critical revision of the article; LMM wrote the manuscript, critical revision of the
358 article; TJR and SWLK provided critical revision of the article; SM and DC analysed data and provided critical
359 revision of the article; JRA analysed data; BSA and AC provided critical revision of the article. All authors
360 provided final approval of the revision to be published.

361 **Online Methods Section**

362 **Experimental set-up**

363 The field experiment was superimposed on an existing biochar study established in October 2006³⁰ (28°49'S,
364 153°23'E, elevation: 140 m). The classification and properties of the topsoil (0-100 mm) are given in Weng et
365 al.¹³. In brief, the rhodic Ferralsol is dominated by kaolinite, gibbsite and goethite mineralogy¹⁶. The soil is
366 acidic (pH 4.5; 0.01 M CaCl₂, 1:5) with 4.5% total C; total Fe 8.4% and total Al 6.7%. The soil was under ryegrass
367 pasture managed for grazing dairy cattle.

368 In April 2014, six square microplots (0.5 m X 0.5 m), using the design by Weng et al.¹³, were superimposed on
369 the existing (at the time, 8.2 years old) trial, with the treatment plots allocated in a randomised complete
370 block design (n=3). The two treatments were 1) 0 t biochar ha⁻¹ ("control"), 2) *E. saligna* biochar (550°C)
371 amendment at 10 t biochar dry weight ha⁻¹ mixed in the top 100 mm of the soil profile in 2006, equivalent to
372 1% w/w ("field-aged biochar"). The physicochemical properties of the biochar are given in Slavich et al.³⁰
373 (Table S3).

374 The microplot area was prepared by mowing existing pasture to remove most of the aboveground biomass.
375 The microplots were open-ended, and edged by heavy duty PVC sheets, 100 mm into the soil, to minimise
376 interference from shallow roots (0-100 mm). To ensure uniformity between microplots, the top 100 mm of
377 unamended or biochar-amended soil was carefully excavated from all microplots, air-dried and manually
378 sieved to less than 2 mm. No stones were found in the soil. Hence the soil was repacked to approximately the
379 same field bulk density of 1.01 g cm⁻³ or 0.99 g cm⁻³ as the unamended or biochar-amended soil, respectively.
380 The soil/biochar mixture was carefully packed into respiration collars to achieve a similar bulk density.

381 Three respiration collars were established at 300 mm into the soils within each microplot, one for soil
382 respiration, one for soil + root respiration and another for root respiration. The description of soil respiration
383 and soil + root respiration collars can be found in Weng et al.¹³. To determine the ¹³C signatures of root
384 respiration, a root signature collar was installed in each of the control microplots and packed with acid-washed
385 sand instead of soil and planted with the same ryegrass. Likewise, a biochar + root signature collar was
386 installed in each of the biochar microplots, which was packed with a mixture of sand and the same hardwood
387 biochar (archived since 2006) at 1% w/w (dry weight basis). Nitrogen fertiliser was applied as urea at 46 kg N
388 ha⁻¹ repeated six times during each winter-spring ryegrass growing season to replicate management of the
389 dairy pasture. For P and K additions, molybdenum superphosphate and muriate of potash were applied
390 annually at 22 kg P ha⁻¹ yr⁻¹ and 50 kg K ha⁻¹ yr⁻¹, respectively. No above ground biomass was present within the
391 respiration collars. The annual ryegrass was harvested monthly and replanted by over sowing, annually.

392 To quantify biochar-plant-soil interactions, three ¹³C pulse labelling campaigns were carried out: 12 June 2014,
393 01 August 2014 and 30 July 2015. The procedure for pulse labelling is described in Weng et al.¹³. Of the six
394 micro-plots within each main plot, three were pulse-labelled with 800 ppmv ¹³CO₂ (99 atom%) and three with
395 800 ppmv ¹²CO₂ as a quality control. Detailed methods of soil aggregate size and SOM fractionation can be
396 found in the supplementary information (SI). Soil microbial metabolic quotient, soil C/¹³C mineralisation rate
397 per unit of microbial C in the biochar-amended and control soils, were determined using the corresponding
398 values of cumulative SOC mineralisation and microbial C for each replicate.

399 The enrichment of ¹³C in solid and gas samples at a specific sampling time (*i.e.* ¹³C_{excess, t}) was calculated (Fig.
400 S3):

$$401 \quad {}^{13}\text{C}_{\text{excess, t}} = {}^{13}\text{C}_{\text{labelled, t}} - {}^{13}\text{C}_{\text{reference}}$$

402 where ¹³C_{labelled, t} is the atom% value of a sample at time t, and ¹³C_{reference} is the average atom% value of the
403 same samples directly before labelling, which is at natural abundance (n=3) (Table S4). To avoid disturbance to
404 the microplots, the ¹³C_{labelled, t} values for soil were only measured at Day 15 after each labelling event (Table
405 S5).

406 The ^{13}C recovery in various C pools at time t (*i.e.* $A^{13}\text{C}_{i,t}$) was calculated by dividing the amount of ^{13}C (g m^{-2}) in
407 a specific C pool (*i.e.* C_i) by the initial amount of total applied $^{13}\text{CO}_2$ (g m^{-2}) at each labelling event (*i.e.* $^{13}\text{C}_{\text{added}}$):

$$408 \quad A^{13}\text{C}_{i,t} = (^{13}\text{C}_{\text{excess},t} \times C_i) / ^{13}\text{C}_{\text{added}} \times 100$$

409 where i = soil + root respiration, root biomass, soil or soil organic matter fraction (Table S6).

410 Details of the sampling and analysis of soil and respiration, and statistical analysis are given in Weng et al.¹³.
411 The hypotheses of equal overall average and equal rate of change (*i.e.* SOC mineralisation, metabolic quotient,
412 substrate-induced respiration, ^{13}C allocation) over time for all treatments were tested using Wald statistics. All
413 statistical analyses were conducted within the R environment (R development core team 2012). When
414 significant F-test results were obtained ($P = 0.05$), mean separation was achieved using a t-test at 0.05
415 probability. Information on SXR, FTIR and XPS analysis of soil and biochar and protocols for catabolic enzyme
416 activities and substrate-induced respiration can also be found in SI.

417 **Calculations of SOC priming in the planted unamended and unplanted biochar-amended soils**

418 The proportion of soil $\text{CO}_2\text{-C}$ in the total $\text{CO}_2\text{-C}$ fluxes from the planted unamended control soil ($C_S(\%)$) was
419 determined using the following two-pool ^{13}C isotopic mixing model¹³:

$$420 \quad C_S(\%) = 100 * (\delta^{13}\text{C}_{T'} - \delta^{13}\text{C}_R) / (\delta^{13}\text{C}_S - \delta^{13}\text{C}_R) \quad (1)$$

421

422 where $\delta^{13}\text{C}_{T'}$ is the $\delta^{13}\text{C}$ signal of the total $\text{CO}_2\text{-C}$ evolved from the planted unamended control soil; $\delta^{13}\text{C}_S$ is the
423 $\delta^{13}\text{C}$ signal of $\text{CO}_2\text{-C}$ evolved from the unplanted unamended controls; and $\delta^{13}\text{C}_R$ is the $\delta^{13}\text{C}$ signature of roots.
424 Root respiration from the root collars (sand) was trapped in 2.5 mL of 2 M NaOH in the dark for 6 h and ^{13}C
425 was analysed as described in Weng et al.¹³.

426 The proportion of soil $\text{CO}_2\text{-C}$ in the total $\text{CO}_2\text{-C}$ fluxes from the unplanted biochar-amended soil ($C_{S''}(\%)$) was
427 determined using the following two-pool ^{13}C isotopic mixing model (see Weng et al.¹³):

$$428 \quad C_{S''}(\%) = 100 * (\delta^{13}\text{C}_{T''} - \delta^{13}\text{C}_B) / (\delta^{13}\text{C}_{S''} - \delta^{13}\text{C}_B) \quad (2)$$

429 where $\delta^{13}\text{C}_{T''}$ is the $\delta^{13}\text{C}$ signal of the total $\text{CO}_2\text{-C}$ evolved from the unplanted biochar-amended soils. $\delta^{13}\text{C}_{S''}$ is
430 the $\delta^{13}\text{C}$ signal of $\text{CO}_2\text{-C}$ evolved from the unplanted controls, and $\delta^{13}\text{C}_B$ is the $\delta^{13}\text{C}$ signature of either fresh (-
431 $25.02 \pm 0.13\text{‰}$) or field-aged biochar ($-25.04 \pm 0.11\text{‰}$). Biochars were extracted manually from the ground,
432 thoroughly washed with demineralised water on a 100 μm sieve and dried at 50°C in an oven for 24 h.

433 We used two baselines to quantify rhizosphere priming in the unamended and biochar-amended systems:

434 i. Unamended system (Planted vs. Unplanted)

435 - $\text{SOC}_{\text{planted, unamended}}$: native SOC mineralisation in the planted unamended system calculated by ^{13}C -
436 enriched root end-member

437 - $\text{SOC}_{\text{unplanted, unamended}}$: native SOC mineralisation in the unplanted unamended system

438

439 Rhizosphere priming in the unamended system:

$$440 \quad \Delta\text{SOC}_{\text{unamended}} = (\text{SOC}_{\text{planted, unamended}}) - (\text{SOC}_{\text{unplanted, unamended}})$$

441 ii. Biochar-amended system (Planted vs. Unplanted)

442 - SOC_{planted, amended}: native SOC mineralisation in the planted biochar-amended system calculated by
443 ¹³C-enriched 'Biochar + Root' end-member

444 - SOC_{unplanted, amended}: native SOC mineralisation in the unplanted biochar-amended system calculated
445 by biochar as one of the end members

446

447 Rhizosphere priming in the biochar-amended system:

448 $\Delta\text{SOC}_{\text{amended}} = (\text{SOC}_{\text{planted, amended}}) - (\text{SOC}_{\text{unplanted, amended}})$

449

450 The priming of native SOC was calculated as the difference in SOC mineralisation within the biochar and
451 control systems:

452 $\Delta\text{SOC} = (C_s(\%)*C_{T_{\text{planted}}} - C_s'(\%)*C_{T_{\text{unplanted}}})/100$ (3)

453 where $C_{T_{\text{planted}}}$ and $C_{T_{\text{unplanted}}}$ are the total CO₂ fluxes in planted biochar-amended and unplanted biochar
454 amended soils for the biochar system; and planted unamended and unplanted unamended soils for the control
455 system.

456 We adapted the calculations of the uncertainty in source partitioning using first order Tyler series
457 approximations of the variances of $C_s(\%)$ ⁵⁵.

458 $\sigma^2 C_s(\%) = (\sigma^2 \delta^{13} C_T - \sigma^2 \delta^{13} C_S) / (\delta^{13} C_T - \delta^{13} C_S)^2$ (4)

459 **Calculated ¹³C atom% (%):**

460 $^{13}\text{C atom\%} = [(\delta^{13}\text{C}+1000)*R_{\text{PDB}}] * 100 / [(\delta^{13}\text{C}+1000)*R_{\text{PDB}}+1]$ (5)

461 where R_{PDB} is the $\delta^{13}\text{C}$ values of Pee Dee Belemnite (PDB), 0.01118.

462 **Aggregate size fractionation**

463 Large macroaggregates (> 2000 μm), small macroaggregates (250-2000 μm), and microaggregates (< 250 μm)
464 were obtained using dry sieving⁵⁶. 50 g of each soil sample was air-dried at room temperature and sieved
465 through 2000 and 250 μm meshes on a FRITSCH vibratory sieve shaker (Analysette 3 Pro, Germany) for 5 min,
466 at an amplitude of 1.5 mm.

467 **Isolation of particulate organic matter (POM) and mineral-protected organic matter**

468 Free POM (f-POM), occluded POM (o-POM) and mineral-bound SOM (m-SOM) were obtained from each
469 aggregate size by methods modified from Gunina and Kuzyakov⁵⁶. To separate f-POM, 5 g of air-dried soil was
470 placed in a 50 mL graduated conical centrifuge tube and 35 mL of 1.6 g cm⁻³ sodium polytungstate (SPT)
471 solution was added. After the tube was gently inverted several times, the solution was centrifuged at 4000
472 rpm for 1 h. The supernatant with floating particles was filtered (cellulose acetate filter, 0.45 μm ; Sartorius,
473 Germany) and washed with distilled water to obtain the f-POM with $\rho < 1.6 \text{ g cm}^{-3}$. SPT was recycled according
474 to Six et al.⁵⁷ to avoid cross contamination of C among fractions.

475 After isolation of f-POM, the aggregates of each size class were dispersed in 0.5% sodium hexametaphosphate
476 by shaking for 18 h on a reciprocal shaker. The dispersed fraction was then passed through 53- μm sieves

477 depending on the original aggregate-size class. The o-POM and mineral-protected SOM (m-SOM) were then
478 isolated.

479 **Microrespirometry Experiment setup (MicroResp™)**

480 Substrate induced respiration was measured using the MicroResp™ method modified from Campbell et al.⁵⁸.
481 The soil samples were air-dried, sieved to below 2 mm, and homogenised by gentle and thorough mixing. Ten
482 treatments were derived in a combination of five doses of biochar at different ages in the presence or absence
483 of plants (Table 1). In our study, fresh biochar amendment did not impact soil pH (data not shown), hence a
484 lime control was not required to balance biochar-induced pH changes on microbial activities. A separate batch
485 of planted and unplanted controls was amended with the same fresh hardwood biochar at 1 % w/w rate to
486 capture the initial change in microbial function after biochar incorporation. Each well of a 96 deep well
487 microtiter plate (1.2 mL; Thermo LifeSciences) was filled with 0.3 g of sample using a filling device described by
488 Campbell et al.⁵⁸. Each field replicate was repeated 8 times. Soil in each well was brought to 40% of water
489 holding capacity (WHC) using distilled water and sealed with parafilm to minimise moisture loss. The soil
490 samples were then incubated in the dark for 7 d before substrate additions to limit the influence from initial
491 disturbance.

492 We selected 15 x C substrates to cover the broad range of C sources which are ecologically relevant to soil
493 based on Campbell et al.⁵⁸, including carbohydrates: N-acetyl-glucosamine, trehalose, L-arabinose
494 (hemicelluloses), D-fructose, D-galactose, glucose, cellobiose; Amino acids: L-alanine, arginine, γ amino Butyric
495 acid, proline; carboxylic acids: citric acid, malic acid, oxalic acid; phenolic acid: protocatechuic acid. The total
496 amount of C in each substrate was delivered as 7.5 mg C per g solution added across all treatments based on
497 the preliminary dose-response trial (data not shown). The sample moisture content was brought to 60% of
498 WHC after C source additions.

499 **Quantification of substrate consumption**

500 To quantify the C substrate consumption in terms of evolved CO₂, a CO₂ absorption microtiter plate containing
501 pH indicating cresol red gel was sealed to the top of the deep well microtiter plate immediately after
502 substrate exposure. The two plates were secured by a metal clip⁵⁸, and incubated for 4.5 h in the dark at 25°C
503 in an incubator with a wet paper towel and soda lime. The absorption plate was read at a wavelength of 540
504 nm on absorbance mode using a fluorescent microplate reader (BMG labtech FLUOstar Omega) at time zero
505 (before substrate dosing) and after 4.5 hours. The absorbance after 4.5 h was normalised for any difference
506 recorded at time zero before exposure and then calibrated against the headspace CO₂ concentration.

507 A calibration curve was established for absorbance versus headspace equilibrium CO₂ concentration by
508 equilibrating dye solutions in gas tight chambers at various CO₂ concentrations diluted from standard gas
509 mixtures (Coregas). The incubation chambers were flushed with argon before standard gas mixtures were
510 introduced. Within each chamber, 4 microtiter wells, detached from breakable CombiStrips (Thermo
511 LifeSciences), were incubated for 4.5 h in the same manner as for the microrespirometry system setup. The
512 headspace CO₂ concentrations were monitored every 2 h during the 4.5 h incubation. After 4.5 h, microtiter
513 wells incubated in different CO₂ gradients were reassembled in a plate carriage to be read as a 96-well plate on
514 a microplate reader. The average amount of evolved CO₂ per sample was calculated and normalised to
515 individual C source concentration.

516 **Enzyme assay in soil suspension**

517 We measured enzyme activity using a soil suspension method^{59,60}. Briefly, 2.5 g of soil was weighed,
518 moistened to 40% WHC, and incubated at 25 °C in a 50 mL centrifuge tube for 7 d. After 7 d incubation, 25 mL
519 of distilled water was dispensed into each centrifuge tube. The soil suspensions were shaken horizontally on
520 an orbital shaker at 200 rpm for 30 min. 100 μ L aliquots of soil suspension were then transferred in triplicate

521 into another 96 deep well microtiter plate prefilled with 900 μL distilled water. The dilution procedure was
 522 repeated once again (*i.e.* 1:100 dilution). 100 μL of the diluted soil suspension was then transferred into a
 523 black 96 well microtiter plate prefilled with 50 μL of modified universal buffer (pH 4)⁶⁰. 100 μL of distilled water
 524 was plated into five wells as hydrolysis blanks. Two standard curves were plotted for each measurement plate:
 525 one for soil (dilution series of 200 μM 4-methylumbelliferyl (MUF) in 50 μL of soil suspension) and the other for
 526 hydrolysis (dilution series of 200 μM MUF in 50 μL of distilled water). 1 mM MUF substrates were prepared
 527 individually for β -glucosidase, cellulase, xylose isomerase and N-acetylglutamate synthase based on Marx et
 528 al.⁵⁹. After adding 50 μL of substrates to soil and hydrolysis wells, the microtiter plate was immediately read at
 529 a wavelength of 450 nm on fluorescence mode using a fluorescent microplate reader (BMG labtech FLUOstar
 530 Omega) as time zero readings. The plates were then placed in an incubator at 37°C and read again after 4.5 h.

531 Sensitivity of C source partitioning

532 The influence of biochar on the $\delta^{13}\text{C}$ signature of soil ($\delta^{13}\text{C}_\text{S}$) has been taken into consideration, due to the
 533 possibility of either positive or negative biochar-induced priming of SOC and/or root-derived C. These
 534 uncertainties of biochar-induced and/or rhizosphere-induced priming on SOC were addressed by partitioning C
 535 sources under three alternative scenarios: 1) extreme positive priming of recent SOC from the current ryegrass
 536 (C_3) pasture by biochar and/or root, which gives $\delta^{13}\text{C}_\text{S}' = -27\text{‰}$ (*i.e.* the upper dashed line in Fig. 2b); 2) equal
 537 magnitude of priming of SOC by biochar and/or root, and labile root C by biochar and/or soil, resulting in
 538 identical soil plus root ^{13}C signatures in the biochar-amended planted soils and the unamended planted soils,
 539 $\delta^{13}\text{C}_\text{S}' = \delta^{13}\text{C}_\text{S}$ (*i.e.* solid triangle in Fig. 2b); and 3) extreme positive priming of the native C_4 -dominant SOC by
 540 biochar and/or root input, which gives $\delta^{13}\text{C}_\text{S+R}' = -13\text{‰}$ (*i.e.* the lower dashed line in Fig. 2b). The ^{13}C parameters
 541 for Scenarios (1) and (3) were based on published values³¹ used to obtain boundary levels. The combination of
 542 95% confidence intervals generated for the lowest and highest scenarios ($n=3$) was used, *i.e.* lower confidence
 543 interval for the lowest scenario and higher confidence interval for the highest scenario. Errors generated from
 544 isotopic partitioning were propagated using the first order Tyler series approximations of the variances of
 545 $\text{C}_\text{S}(\%)$ ⁵⁵.

$$546 \sigma^2 \text{C}_\text{S}(\%) = (\sigma^2 \delta^{13}\text{C}_\text{T} - \sigma^2 \delta^{13}\text{C}_\text{S}) / (\delta^{13}\text{C}_\text{T} - \delta^{13}\text{C}_\text{S})^2 \quad (4)$$

547 Biometrical analysis

548 The responses of SOC mineralisation, metabolic quotient, substrate-induced respiration and ^{13}C allocation to
 549 the experimental design and seasonal factors were assessed by fitting linear mixed models. These were
 550 designed to account for variability in each response due to treatment and temporal trends plus random effects
 551 due to replicates and plots within replicates plus random event-driven effects associated with each sampling
 552 date. After fitting the model for each variable, the hypotheses of equal overall average and equal rate of
 553 change (*i.e.* SOC mineralisation, metabolic quotient, substrate-induced respiration, ^{13}C allocation) over time for
 554 all treatments were tested using Wald statistics. The models were then used to estimate the average response
 555 under each treatment interpolated to daily measurements. After C source partitioning, the cumulative SOC
 556 mineralisation from 8.2 to 9.5 years was calculated as the area of a linear interpolation across all measurement
 557 points in the biochar-amended and unamended control soils. The extent of biochar-induced priming effect of
 558 SOC was quantified as the difference between the biochar-amended SOC mineralisation and the control SOC
 559 mineralisation in the presence or absence of plants. These results were presented in graphical form in Excel,
 560 bounded by twice the estimated SE of the predictions to estimate 95% confidence intervals. All statistical
 561 analyses were conducted within the R environment⁶¹ including the linear modelling tools available from the
 562 Asreml R package⁶³. When significant F-test results were obtained ($P=0.05$), mean separation was achieved
 563 using a t-test at the 0.05 probability level.

564 Extrapolation of extra biochar C sequestration potential in (sub)tropical pasture on Ferralsol

565 Biochar production may reach 5.5 to 9.5 Gt per year in 2100⁵³ and 87% of the feedstock for the current biochar
566 production is wood⁶³. Assuming the same proportion in 2100, the amount of woody biochar available would
567 be 4.8 - 8.3 Gt. At 10 t ha⁻¹, an area of 0.5 - 0.8 Gha could be amended in 2100. This area would occupy 64-
568 100% of tropical Ferralsols, or 22-36% of tropical savannas and grasslands⁵². The C sequestration potential in
569 grasslands is estimated to reach a global average of 5.4 X 10⁻¹⁰ Pg C ha⁻¹ yr⁻¹ by 2100¹. Assuming all woody
570 biochar produced in 2100 was applied to grassland (*i.e.* 0.5 to 0.8 Gha), upper range limits (based on the
571 average) of C sequestration in grasslands before biochar amendment in 2100 would be around 0.27-0.43 Pg C
572 (*i.e.* 0.5 or 0.8 Gha multiplies 5.4 X 10⁻¹⁰ Pg C ha⁻¹ yr⁻¹). We showed a 10% increase in SOC stabilisation in the
573 9.5-year-aged biochar-amended soil *cf.* the unamended control. This would result in an additional C
574 sequestration potential of 0.03-0.04 Pg C by 2110 (*i.e.* 10% multiplies 0.27 or 0.43 Pg C).

575 **Experimental Method: Soft X-ray (SXR), Fourier Transform Infrared Spectroscopy (FTIR) and X-ray** 576 **photoelectron spectroscopy (XPS)**

577 Synchrotron based near edge X-ray absorption fine structure (NEXAFS) was implemented at the Soft X-ray
578 Spectroscopy beamline (14ID) at the Australian Synchrotron (AS). The soft X-ray beamline consists of an
579 elliptically polarising undulator and plane grating monochromator using a grating of 1200 l/m. The nominal
580 beam size was 0.15x0.015 mm at the sample. The light was linearly polarised. The synchrotron was operated
581 in continuous top-up mode. The end-station was constructed by Omni Vac and PreVac and equipped with a
582 SPECS Phoibos 150 electron energy analysis and Omni Vac UHV-compatible partial yield detector based on a
583 multichannel plate behind retarding grids. NEXAFS C K-edge spectra were collected using drain current and
584 total fluorescence yield (TFY). The beamline grating exit slits were set to 20 µm providing a calculated energy
585 resolution of 0.05 eV at a photon energy of 280 eV.

586 The spectra were collected over a photon energy range of 275 to 325 eV with a step size of 0.1 eV. The spectra
587 were collected at an angle of 100° to the beam. The energy calibration was carried out using a graphite
588 standard in the beamline which was collected simultaneously with the IO and sample NEXAFS spectra. The
589 spectra were normalised to the IO and a photodiode measurement, collected in the UHV analytical chamber.
590 The normalisation was carried out using the double normalization method described by Stöhr⁶⁴. The
591 background normalisation was carried out using a pre and post-edge linear subtraction and the Athena
592 software. The samples were pre-ground to a fine powder and mounted on double sided C or copper tape
593 affixed to a stainless steel disk.

594 FTIR spectra were acquired using a Nicolet 6700 FTIR spectrometer (Thermo Fisher Scientific Inc., Waltham,
595 MA, USA) equipped with a KBr beam-splitter. Absorption spectra of bulk soils were trimmed from 600 - 4000
596 cm⁻¹ to obtain the MIR spectral region.

597 The X-ray photoelectron analyses were performed in an ultra-high vacuum station (Escapulus P System,
598 Omicron Nanotechnology, Taunusstein, Germany), with pressure in the measurement chamber of 10⁻¹⁰ mbar,
599 using an Mg X-ray source (K=1253.6 eV), with power given by emission of 18 mA, at a voltage of 15 kV. For the
600 individual peak regions, we used an analyser with pass energy of 20 eV and a step of 0.05 eV. Survey spectrum
601 was measured at 100 eV analyser pass energy. The binding energies were referred to the C 1s levels, set as
602 284.6 eV. Analyses of the peaks were performed with the CasaXPS software, using a weighted sum of
603 Lorentzian and Gaussian components curves after performing a Shirley background subtraction.

604 **Data availability**

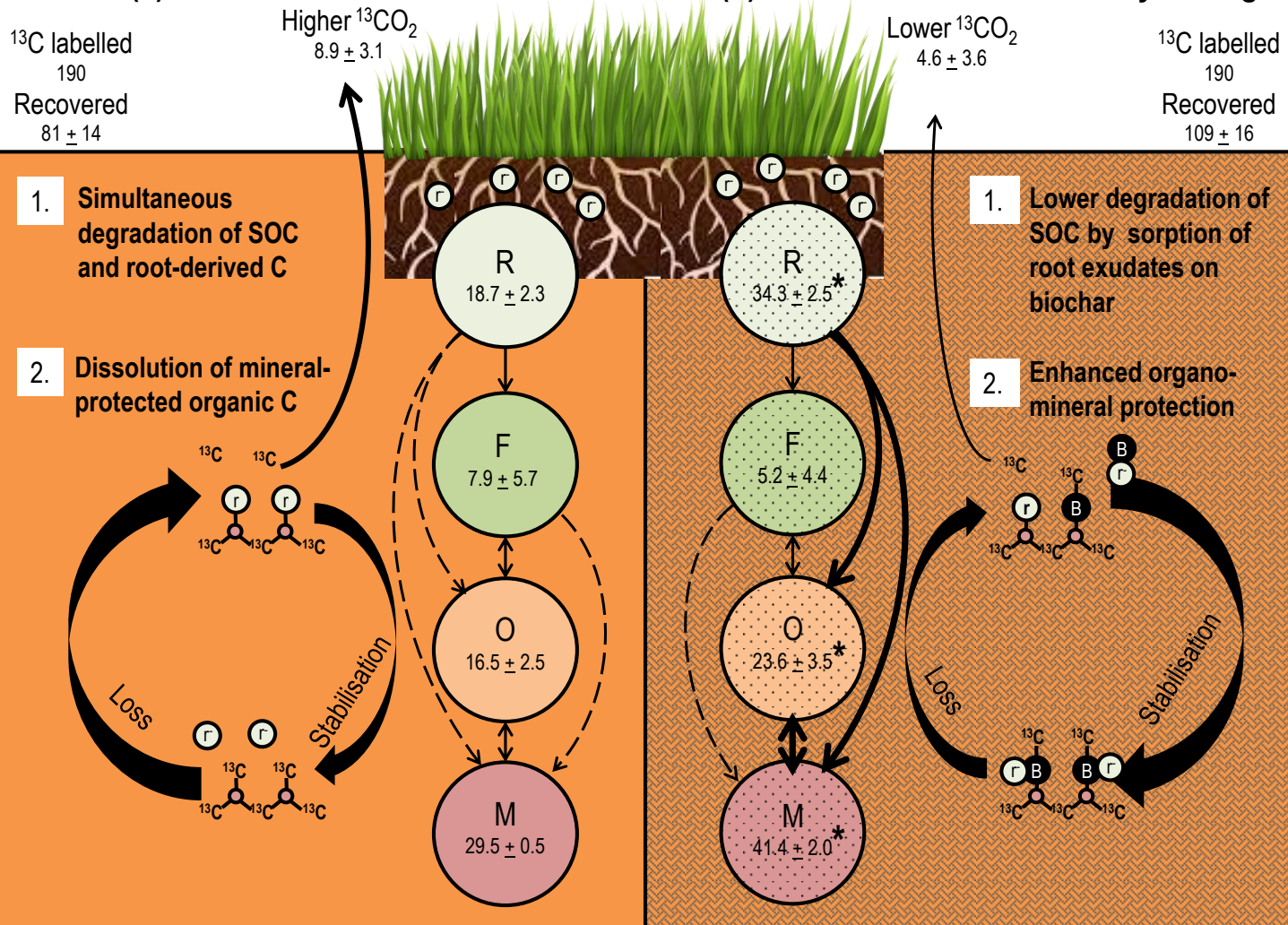
605 The authors declare that the ¹³C raw data of soil and CO₂ and results of belowground C allocation, XPS analysis
606 on field-extracted biochar, aboveground biomass and microbial analysis supporting the findings of this study
607 are available within the article and its supplementary information files. The rest of data that support the
608 findings of this study are available from the corresponding author upon request.

609 **Reference**

- 610 55 Derrien, D. *et al.* Does the addition of labile substrate destabilise old soil organic matter? *Soil Biology and*
611 *Biochemistry* **76**, 149-160, doi:<http://dx.doi.org/10.1016/j.soilbio.2014.04.030> (2014).
- 612 56 Gunina, A. & Kuzyakov, Y. Pathways of litter C by formation of aggregates and SUM density fractions: Implications
613 from C-13 natural abundance. *Soil Biology & Biochemistry* **71**, 95-104, doi:10.1016/j.soilbio.2014.01.011 (2014).
- 614 57 Six, J., Elliott, E. T., Paustian, K. & Doran, J. W. Aggregation and soil organic matter accumulation in cultivated and
615 native grassland soils. *Soil Science Society of America Journal* **62**, 1367-1377 (1998).
- 616 58 Campbell, C. D., Chapman, S. J., Cameron, C. M., Davidson, M. S. & Potts, J. M. A rapid microtiter plate method to
617 measure carbon dioxide evolved from carbon substrate amendments so as to determine the physiological
618 profiles of soil microbial communities by using whole soil. *Applied and Environmental Microbiology* **69**, 3593-
619 3599 (2003).
- 620 59 Marx, M.-C., Wood, M. & Jarvis, S. A microplate fluorimetric assay for the study of enzyme diversity in soils. *Soil*
621 *Biology and Biochemistry* **33**, 1633-1640 (2001).
- 622 60 Turner, B. L. Variation in pH optima of hydrolytic enzyme activities in tropical rain forest soils. *Applied and*
623 *Environmental Microbiology* **76**, 6485-6493 (2010).
- 624 61 R Development Core Team. R: A language and environment for statistical computing. R Foundation for Statistical
625 Computing. Vienna, Austria. ISBN 3-900051-07-0, URL <http://www.R-project.org> (2012).
- 626 62 Butler, T., Dawson, C., Wildey, T. A POSTERIORI ERROR ANALYSIS OF STOCHASTIC DIFFERENTIAL EQUATIONS
627 USING POLYNOMIAL CHAOS EXPANSIONS. *Siam Journal on Scientific Computing* **33**, 1267-1291 (2011).
- 628 63 IBI. 2013 State of the Biochar Industry: A Survey of Commercial Activity in the Biochar Field. International Biochar
629 Initiative. p. 1–61. [http://www.biochar-](http://www.biochar-international.org/sites/default/files/State_of_the_Biochar_Industry_2013.pdf)
630 [international.org/sites/default/files/State_of_the_Biochar_Industry_2013.pdf](http://www.biochar-international.org/sites/default/files/State_of_the_Biochar_Industry_2013.pdf) (2014)
- 631 64 Stöhr, J. *NEXAFS spectroscopy*. Vol. 25 (Springer Science & Business Media, 2013).

(a) Unamended control

(b) Amended with biochar 9.5 years ago



Belowground ^{13}C pools:

- (R)** Root biomass (and its exudates)
- (F)** Free particulate organic matter
- (O)** Occluded particulate organic matter
- (M)** Mineral fractions
- (B)** Biochar

Carbon output, in $\text{mg } ^{13}\text{CO}_2\text{-C m}^{-2}$

Numbers indicate new C retention in each pool with 1 SE, in $\text{mg } ^{13}\text{C m}^{-2}$

Mineral-protected new C

Chemically reduced rhizodeposits

Figure 1 Proposed mechanisms for positive rhizosphere priming of soil organic carbon (SOC) counteracted by biochar-induced negative priming and stabilisation of rhizodeposits (new C) in a Ferralsol after 9.5 years. In the planted controls (Fig. 1a), 1) chemically reduced root exudates can stimulate simultaneous degradation of native SOC and new root-derived C, thus increasing mineralisation of SOC (positive priming); 2) root exudates may also cause dissolution of mineral-protected organic C and complexation of fixed Fe^{3+} via ligand exchange²⁶, which increases bioavailability of mineral-bound SOC to microbial consumption. Contrastingly, despite the co-occurrence of these two mechanisms in the planted biochar-amended soil (Fig. 1b), 1) biochar sorbs root exudates, hence minimizing dissolution of iron as well as mineral-protected organic C, which may lower SOC mineralisation; 2) biochar can serve as ligand to enhance organo-mineral interactions, which results in stabilising new C. The arrows illustrate the C flow directions (i.e. single arrow: unidirectional; dual arrow: interchangeable). Dashed arrows indicate negligible C flow between pools. * indicates significant difference in C pools between soil fractions by t-test , $P < 0.05$.

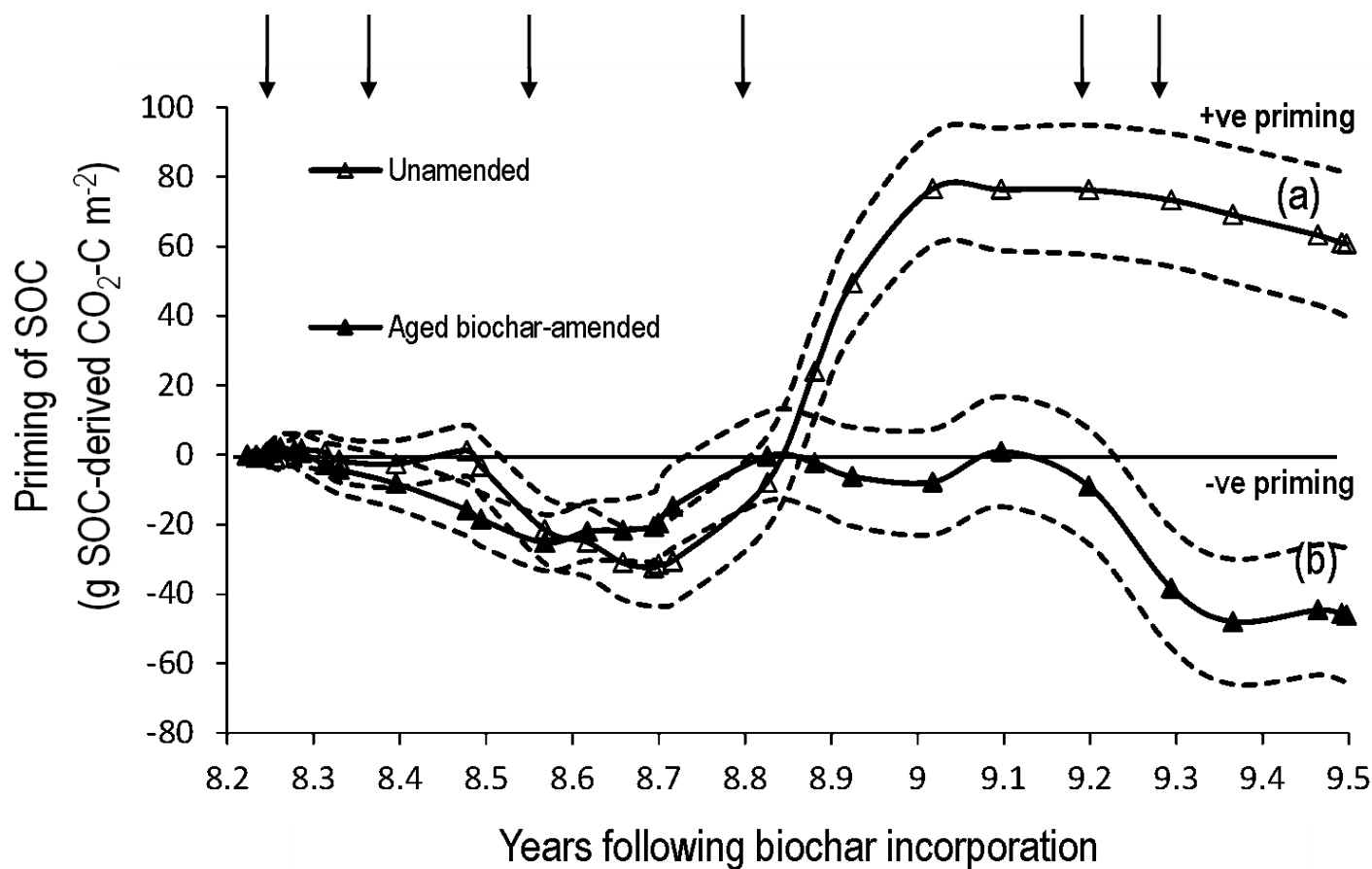


Figure 2: **Rhizosphere priming of soil organic carbon (SOC) as difference of cumulative SOC mineralisation between (a) planted and unplanted unamended controls; (b) planted biochar-amended and unplanted biochar-amended soil.** Confidence intervals (95% CI) of rhizosphere priming in both unamended and biochar amended systems are plotted in dashed lines and normalised against the mean squares across all treatments at each sampling event (n= 3). For biochar amendment, the CI was based on a sensitivity analysis (Online Method Section), which considers the extreme scenarios of contrasting SOC pools (C₃ vs. C₄-dominated) by differences in δ¹³C signatures. The six arrows represent N fertiliser additions.

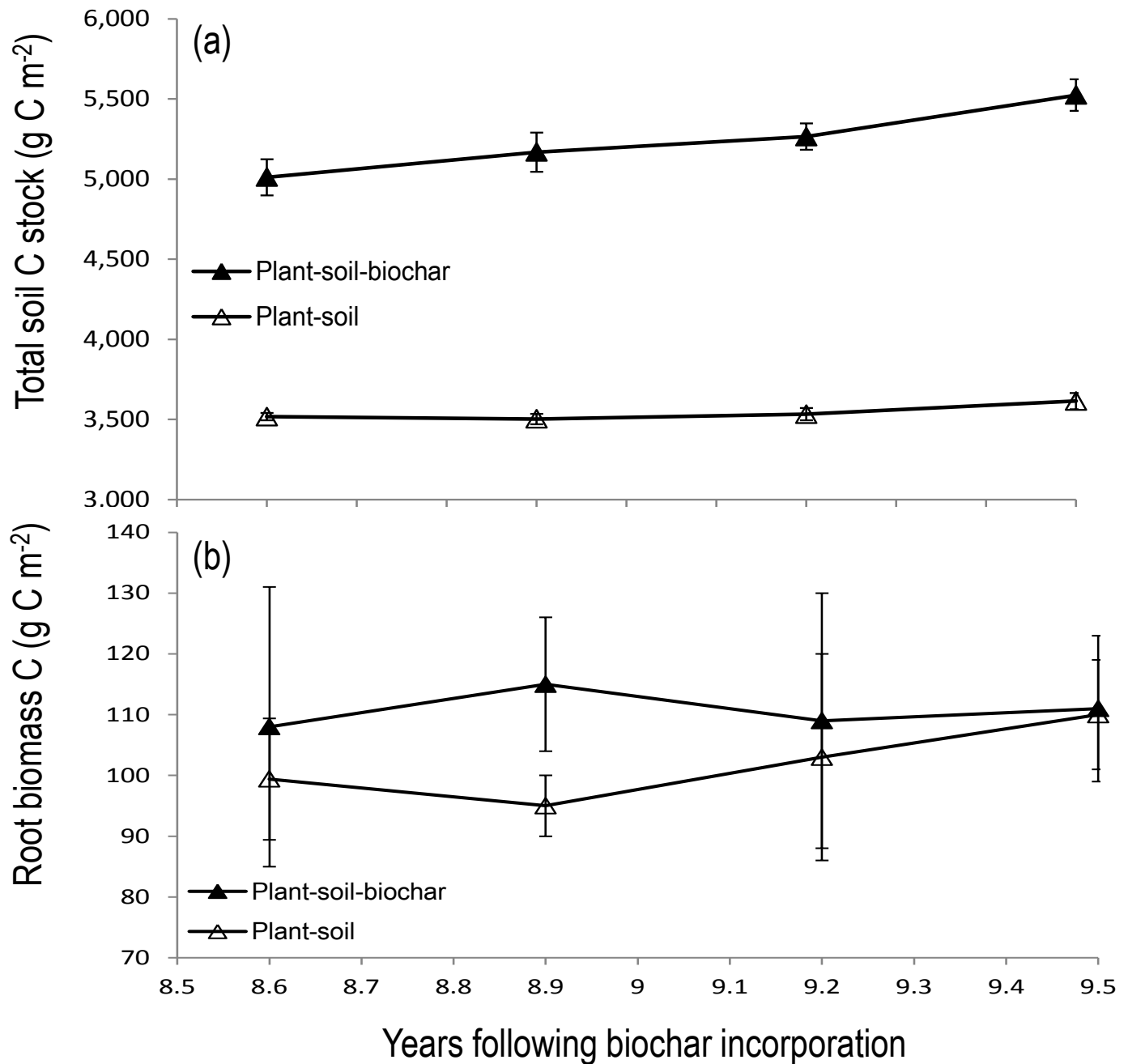


Figure 3: **Total soil C stocks (a) and root biomass C (b) measured at 4-month intervals in the unamended control and field-aged biochar-amended plots.** The total soil C content was adjusted against the field bulk density and sampling depth (i.e. 0-100 mm) at each sampling time. Standard error bars are provided (n=3).

(a) SXR of bulk planted soils

(b) FTIR of bulk planted soils

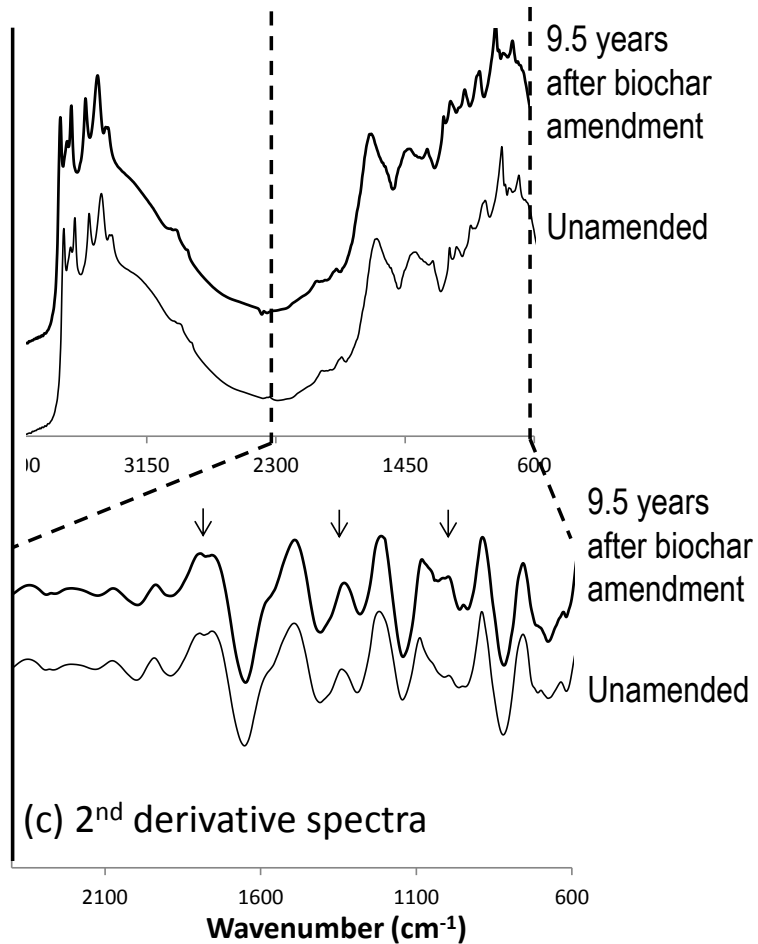
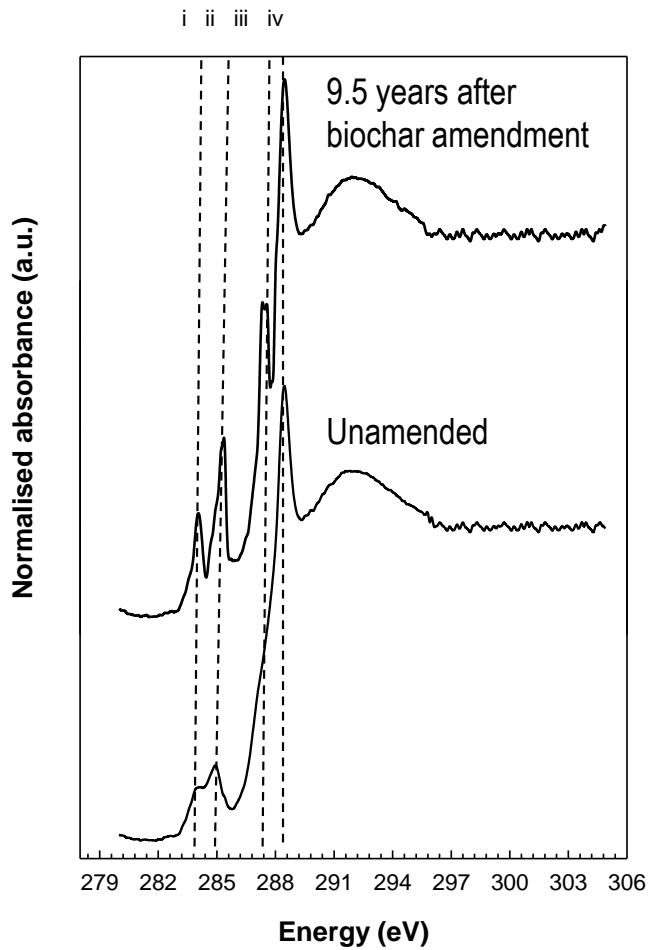


Figure 4: (a) **Average SXR spectra of bulk planted soils** with or without biochar amendment (n=9, CV% <3.2%); (b) **Average FTIR spectra of bulk planted soils** with or without biochar amendment; (c) **Average 2nd derivative spectra of FTIR**

1 **Supplementary information (SI)**

2 **Biochar built soil carbon over a decade by stabilising** 3 **rhizodeposits**

4 Zhe (Han) Weng^{1,2}, **Lukas Van Zwieten**^{1,3,4★}, Bhupinder Pal Singh^{1,5}, Ehsan Tavakkoli^{2,6},
5 Stephen Joseph^{7,8,9}, Lynne M. Macdonald¹⁰, Terry J. Rose⁴, Michael T. Rose³,
6 Stephen W. L. Kimber³, Stephen Morris³, Daniel Cozzolino¹¹, Joyce R. Araujo¹², Braulio S
7 Archanjo¹² and Annette Cowie^{1,13}

8 1 School of Environmental and Rural Sciences, University of New England, Armidale, NSW 2351

9 2 Graham Centre for Agricultural Innovation, Charles Sturt University, Wagga Wagga NSW 2650

10 3 NSW Department of Primary Industries, Wollongbar Primary Industries Institute, Wollongbar, NSW 2477

11 4 Southern Cross University, East Lismore, NSW 2480

12 5 NSW Department of Primary Industries, Elizabeth Macarthur Agricultural Institute, Woodbridge Rd, Menangle, NSW 2568

13 6 NSW Department of Primary Industries, Wagga Wagga Agricultural Institute, Wagga Wagga NSW 2650

14 7 University of Newcastle, Callaghan, NSW 2308

15 8 University of New South Wales, Sydney, NSW 2052

16 9 University of Wollongong, Wollongong, NSW 2522

17 10 CSIRO Agriculture, Waite campus, Glen Osmond, SA 5064

18 11 Central Queensland Innovation and Research Precinct, North Rockhampton, Central Queensland University, QLD 4701

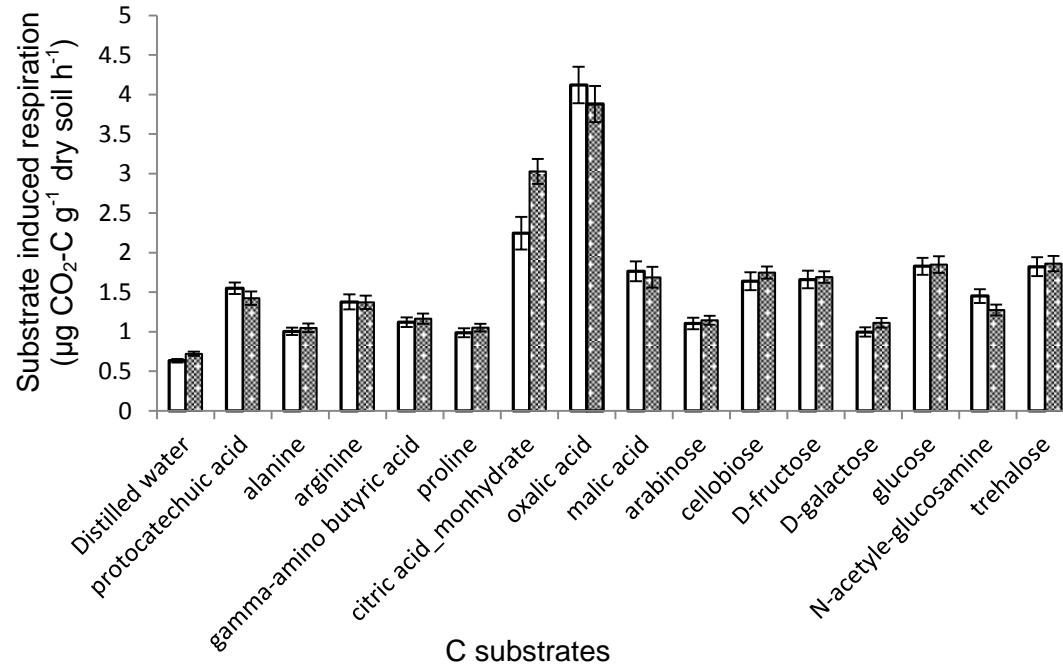
19 12 Divisão de Metrologia de Materiais - DIMAT, Instituto Nacional de Metrologia, Normalização e Qualidade Industrial -
20 INMETRO, Duque de Caxias, RJ, 25250-020, Brazil

21 13 NSW Department of Primary Industries, Armidale, NSW 2351

22 ★Email: lukas.van.zwieten@dpi.nsw.gov.au

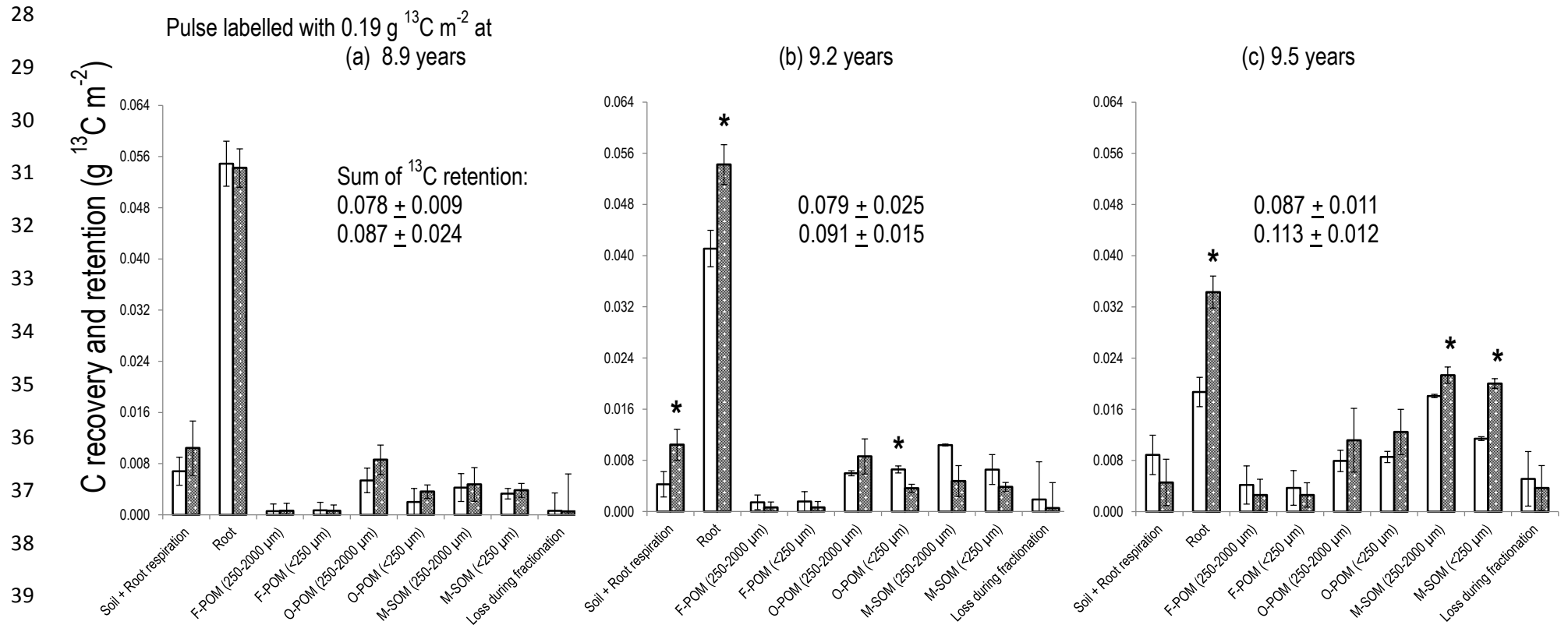
23 **Figures**

24



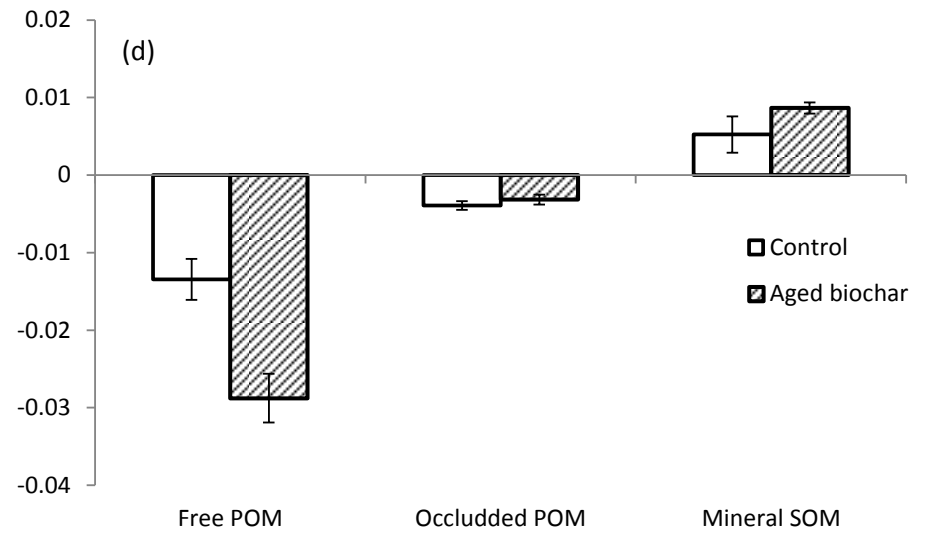
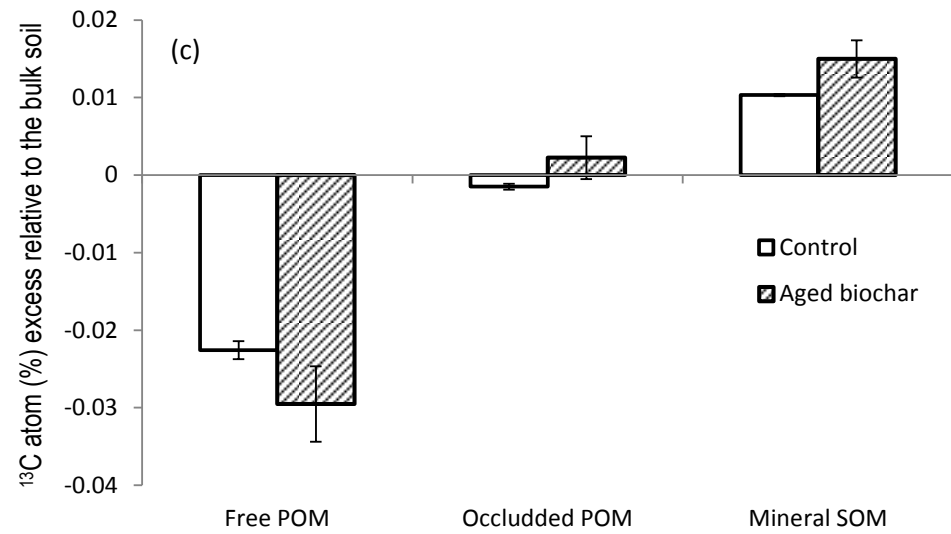
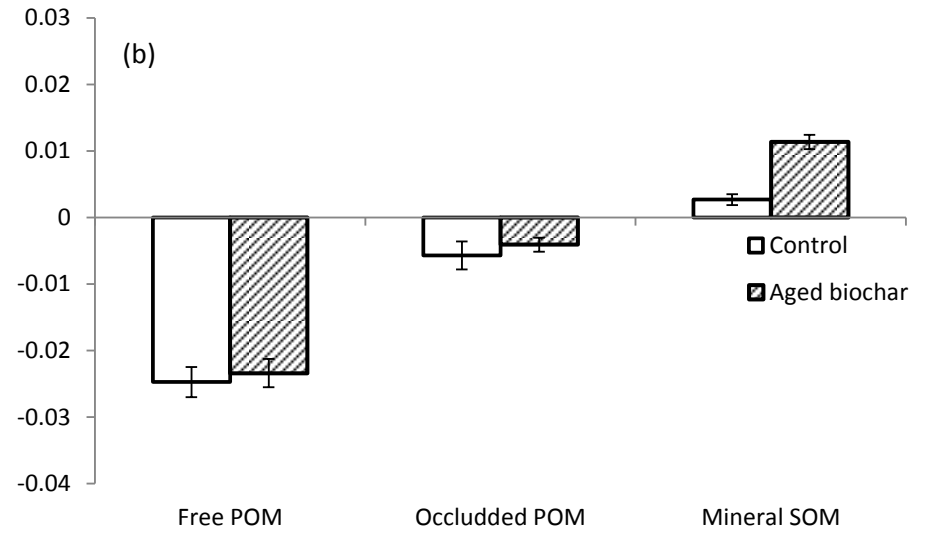
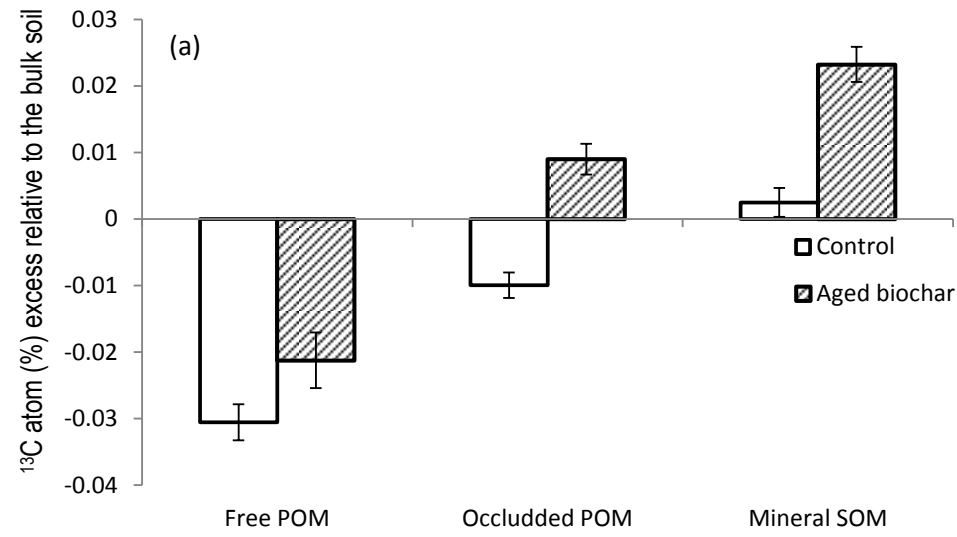
25

26 *Figure S1: Substrate induced respiration in planted control (open) and 9.5-year biochar-amended (dark) soils (9.5 years) using 15 C substrates (standardised*
27 *7.5 mg C) based on Microresp[®]. Distilled water used as a blank. Standard errors are plotted as error bars (n=24). Standard error bars are provided.*



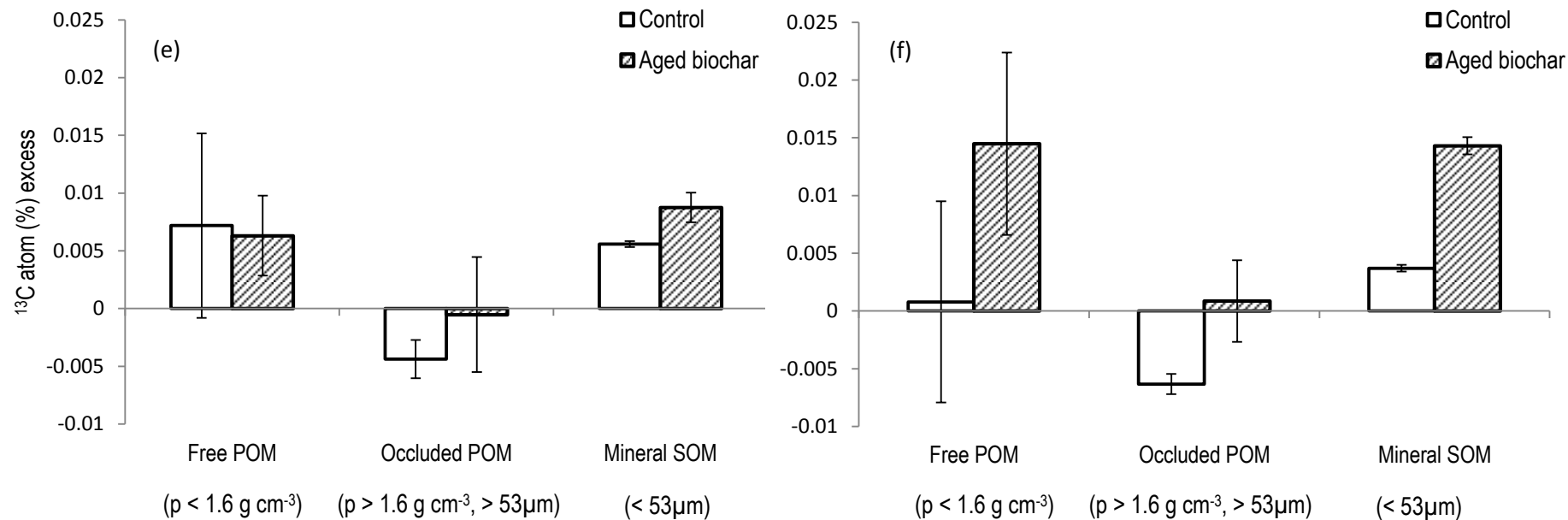
Belowground C pools

Figure S2: Belowground ^{13}C recovery and retention (0-100 mm) in different C pools in control and biochar soils on Day 15 at 8.9- (a), 9.2- (b) and 9.5- (c) year pulse labelling event. Each labelling event was allocated with the same amount enrichment of $0.19 \text{ g } ^{13}\text{C m}^{-2}$. Standard errors are given ($n=3$). F-POM: free particulate organic matter; O-POM: occluded particulate organic matter; M-SOM: mineral soil organic matter. Sum of ^{13}C retention in $\text{g } ^{13}\text{C m}^{-2}$ for each event was also given, top numbers for control and bottom ones for biochar soils. *, $P < 0.05$.



46

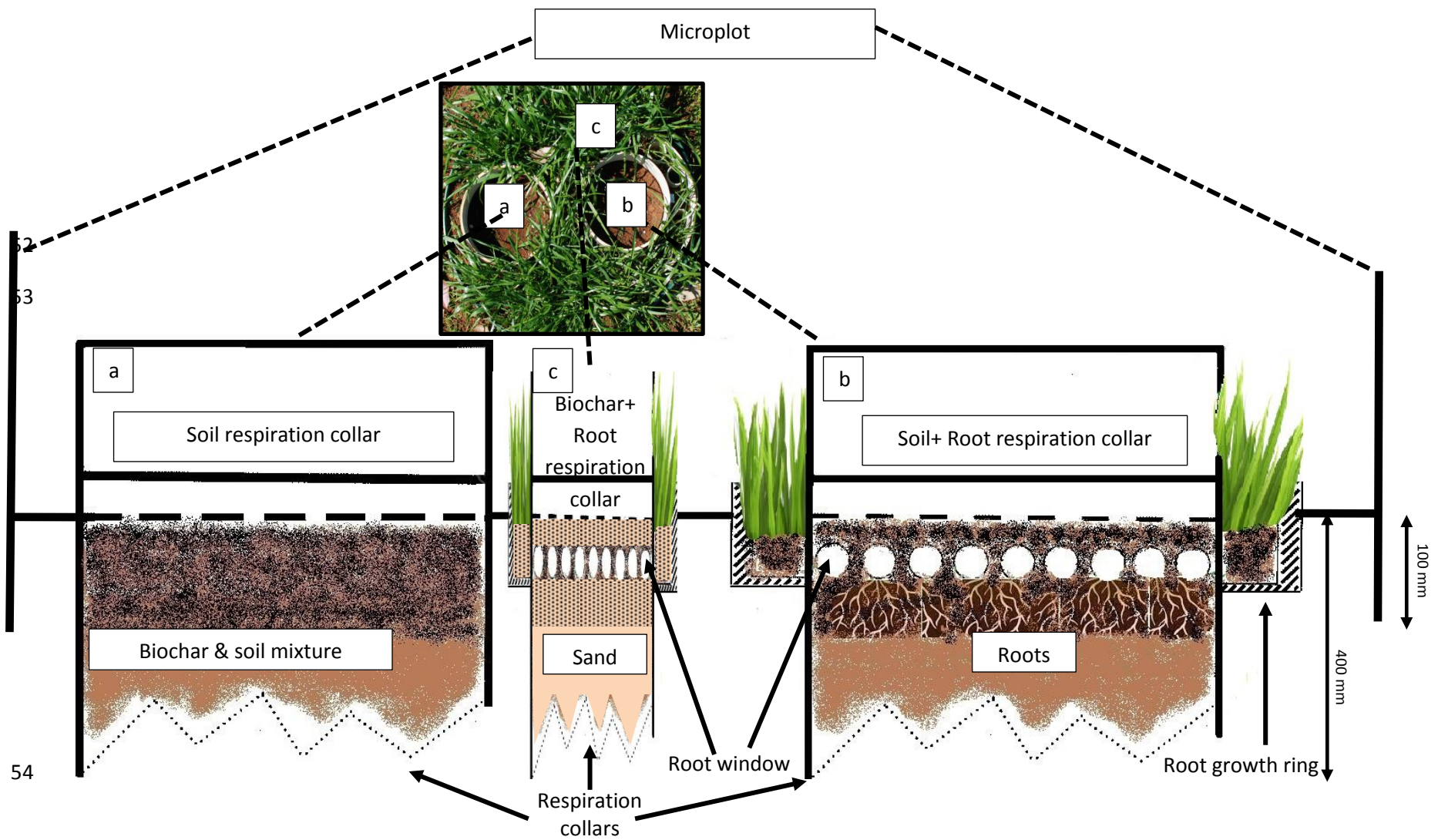
47



48

49

50 *Figure S3: ^{13}C atom (%) excess relative to the bulk soil within each soil fraction of control and biochar-amended macroaggregates and microaggregates at*
 51 *8.9- ((a) & (b)), 9.2- ((c) & (d)) and 9.5- (e) & (f)) year pulse labelling event. Standard errors are plotted as error bars (n=3).*



55 *Figure S4: A photograph of one microplot is shown. A cross section of (a) the soil respiration, (b) soil plus root respiration and (c) biochar plus root collars in a*
 56 *biochar-amended microplot are presented (Bottom). The area outside the respiration collars is planted with an annual ryegrass.*

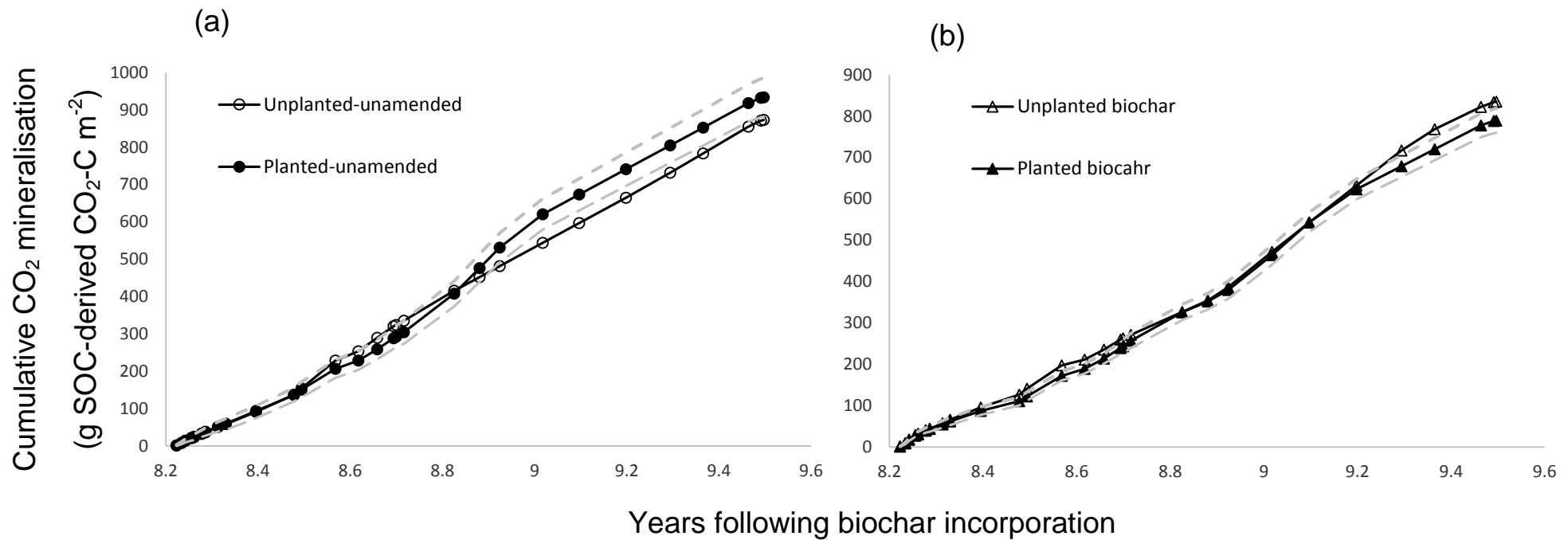


Figure S5: Cumulative SOC mineralisation in the unamended (unplanted and planted) and biochar-amended (unplanted and planted) systems. Note that the unplanted systems were only unplanted between 8.2-9.5 years after incorporation. Before that period, the systems were under pasture management. There is still residual root-C in the unplanted systems. Confidence intervals (95%CI) of cumulative CO₂ efflux of planted unamended and planted biochar-amended are plotted in dashed lines and normalised against the mean squares across all treatments at each sampling event (n= 3).

57 **Tables**

58 *Table S1: Metabolic quotient as microbial respiration (from total C and rhizodeposits, ¹³C) over microbial biomass carbon (MBC) in control and biochar soils*
 59 *(9.5 years) at 8.9-, 9.2- and 9.5-year pulse labelling time. SE presented (n=3, *, significant difference in metabolic quotient between biochar-amended and*
 60 *unamended control soil, P< 0.05).*

	Metabolic quotient ($\mu\text{g CO}_2\text{-C mg}^{-1}\text{ MBC h}^{-1}$)					
	8.9 years		9.2 years		9.5 years	
	Mean	SE	Mean	SE	Mean	SE
Control	1.22	0.04	0.755	0.053	0.287*	0.022
Biochar	1.22	0.07	0.784	0.092	0.158	0.053

	Metabolic quotient of rhizodeposits ($\text{ng } ^{13}\text{CO}_2\text{-}^{13}\text{C mg}^{-1}\text{ MBC h}^{-1}$)					
	8.9 years		9.2 years		9.5 years	
	Mean	SE	Mean	SE	Mean	SE
Control	1.47	0.22	0.081	0.0071	0.300	0.034
Biochar	1.98	0.43	0.103	0.0063	0.307	0.022

61 *Table S2: Enzyme activities of β -glucosidase (Glc), xylosidase (Xyl), cellulase (Cel), N-acetyl-glucosaminidase (Nag) in planted unamended control and planted*
 62 *biochar-amended soils sampled at Year 9.5 (nmol methylumbelliferone g^{-1} dry soil h^{-1}). SE presented (n= 24).*

	Glc		Cel		Nag		Xyl	
	Mean	SE	Mean	SE	Mean	SE	Mean	SE
Control	179	32.1	35.7	10.2	122	22.7	48.5	4.83
Biochar	162	20.7	23.6	2.8	118	18.8	53.3	8.83

63

64 Table S3: The chemical properties of biochar and soil. Details of the analytical procedures can also be found in Slavich et al. (2013).

Properties	Units	<i>Eucalyptus saligna</i> biochar (550°C)	Ferralsol
$\delta^{13}\text{C}$	‰	-25.02	-20.23
Total C	%	76	4.69
Total N	%	0.20	3.31
CEC	cmol _c kg ⁻¹	1.2	5.2
pH (1:5 H ₂ O)		7.83	4.09

65

66 Table S4: Time sequence of the excess of enriched ¹³C values of respiration and root biomass relative to ¹³C values of respiration and root biomass at natural
67 abundance in control and field-aged biochar-amended soils at 8.9- (a), 9.2- (b) and 9.5- (c) year pulse labelling event (n=3). Standard errors are presented.

(a)		Control							
Days after 8.9-year labelling		3		5		10		15	
¹³ C excess (atom%)		Mean	SE	Mean	SE	Mean	SE	Mean	SE
Soil + Root respiration		0.0134	0.0061	0.0684	0.0306	0.0949	0.0216	0.1257	0.0349
Root		0.1001	0.0055	0.0869	0.0050	0.0512	0.0073	0.0554	0.0035
		Field-aged biochar							
Days after 8.9-year labelling		3		5		10		15	
¹³ C excess (atom%)		Mean	SE	Mean	SE	Mean	SE	Mean	SE
Soil + Root respiration		0.0226	0.0057	0.0085	0.0102	0.1225	0.0405	0.1650	0.0528
Root		0.0863	0.0058	0.0773	0.0058	0.0516	0.0062	0.0547	0.0036

(b)		Control							
Days after 9.2-year labelling	3		5		10		15		
¹³ C excess (atom%)	Mean	SE	Mean	SE	Mean	SE	Mean	SE	
Soil + Root respiration	0.0064	0.0057	0.0310	0.0372	0.0275	0.0197	0.0160	0.0178	
Root	0.0795	0.0093	0.0744	0.0068	0.0512	0.0140	0.0415	0.0029	
		Field-aged biochar							
Days after 9.2-year labelling	3		5		10		15		
¹³ C excess (atom%)	Mean	SE	Mean	SE	Mean	SE	Mean	SE	
Soil + Root respiration	0.0041	0.0061	0.0722	0.0408	0.0345	0.0295	0.0176	0.0107	
Root	0.0822	0.0030	0.0788	0.0009	0.0334	0.0027	0.0415	0.0091	

68

(c)		Control							
Days after 9.5-year labelling	3		5		10		15		
¹³ C excess (atom%)	Mean	SE	Mean	SE	Mean	SE	Mean	SE	
Soil + Root respiration	0.0239	0.0104	0.0770	0.0051	0.0940	0.0628	0.1007	0.0365	
Root	0.0802	0.0050	0.0720	0.0093	0.0579	0.0023	0.0189	0.0033	
		Field-aged biochar							
Days after 9.5-year labelling	3		5		10		15		
¹³ C excess (atom%)	Mean	SE	Mean	SE	Mean	SE	Mean	SE	
Soil + Root respiration	0.0168	0.0126	0.0662	0.0057	0.1991	0.0640	0.1246	0.0296	
Root	0.0851	0.0026	0.0723	0.0058	0.0498	0.0027	0.0347	0.0063	

69

70 *Table S5: Excess of enriched ¹³C values of bulk soil and soil fractions relative to ¹³C values of bulk soil and soil fractions at natural abundance in control and*
 71 *field-aged biochar-amended soils on Day 15 of 8.9-, 9.2- and 9.5-year pulse labelling event (n=3). Standard errors are presented.*

¹³ C excess (atom%)	Day 15 of 8.9-year labelling				Day 15 of 9.2-year labelling				Day 15 of 9.5-year labelling			
	Control		Field-aged biochar		Control		Field-aged biochar		Control		Field-aged biochar	
	Mean	SE	Mean	SE	Mean	SE	Mean	SE	Mean	SE	Mean	SE
Bulk soil	1.55E-03	6.64E-04	1.15E-03	2.49E-04	7.30E-04	4.29E-04	5.94E-04	1.37E-04	1.27E-03	2.12E-04	1.00E-03	1.75E-04
Free POM (250-2000 μm)	6.08E-04	2.72E-04	5.43E-04	4.17E-04	1.39E-03	1.15E-04	1.10E-03	4.86E-04	3.79E-03	7.99E-04	2.35E-03	3.46E-04
Free POM (<250 μm)	7.41E-04	2.27E-04	5.48E-04	2.12E-04	1.52E-03	2.64E-04	9.63E-04	3.14E-04	3.38E-03	8.71E-04	2.35E-03	7.90E-04
Occluded POM (250-2000 μm)	1.15E-04	1.92E-04	1.25E-04	2.30E-04	1.27E-04	3.84E-05	8.94E-05	2.76E-04	1.65E-04	1.66E-04	1.52E-04	4.98E-04
Occluded POM (<250 μm)	4.32E-05	2.11E-05	5.25E-05	1.04E-04	1.39E-04	5.51E-05	7.98E-05	6.37E-05	1.77E-04	8.81E-05	1.69E-04	3.54E-04
Mineral SOM (250-2000 μm)	9.14E-05	2.18E-05	6.91E-05	2.64E-05	2.21E-04	1.44E-05	1.85E-04	2.41E-04	3.75E-04	2.51E-05	2.90E-04	1.28E-04
Mineral SOM (<250 μm)	7.08E-05	8.22E-05	5.55E-05	1.09E-05	1.39E-04	2.34E-04	1.74E-04	7.20E-05	2.37E-04	2.96E-05	2.72E-04	7.50E-05

72

73 *Table S6: Proportion of belowground ¹³C allocation relative to the total allocated ¹³C enrichment (in percentage) within control and field-aged biochar-*
 74 *amended Soil + Root respiration collars at 8.9-, 9.2- and 9.5-year pulse labelling time. Standard errors are given (n=3).*

	Pulse labelling at	8.9-year time				9.2-year time				9.5-year time			
		Control	SE	Biochar	SE	Control	SE	Biochar	SE	Control	SE	Biochar	SE
Soil + Root respiration	(%)	3.67	0.219	5.61	0.425	2.29	0.197	4.37	0.241	4.77	0.308	2.46	0.363
Root	(%)	29.5	1.89	29.2	1.61	22.1	1.53	22.1	4.86	10.1	2.30	18.5	2.51
Soil	(%)	9.03	1.67	12.5	9.23	18.5	10.9	22.4	5.17	31.7	5.48	39.8	6.94

75

76 *Table S7: Redox potentials, pH, mineral N, Fe²⁺ and Fe³⁺ and water and solid P content of control and biochar-amended soil in the presence or absence of*
 77 *plants at 9.5-year pulse labelling event. Standard errors are given (n=3).*

		Unplanted		Planted	
		Mean	SE	Mean	SE
Eh (mV)	Control	577	1.8	585	7.1
	Biochar	618	13	623	14
pH (1:5 H ₂ O)	Control	4.16	0.15	3.85	0.05
	Biochar	4.06	0.09	4.09	0.07
KCl Extractable Ammonium-N (mg kg ⁻¹)	Control	20.0	5.69	53.7	7.31
	Biochar	22.0	5.69	88.7	5.93
KCl Extractable Nitrate-N (mg kg ⁻¹)	Control	53.7	15.6	98.3	13.0
	Biochar	70.0	10.4	130	5.77
HCl extractable Fe ²⁺ (mmol kg ⁻¹)	Control	0.256	0.001	0.248	0.0001
	Biochar	0.252	0.002	0.246	0.0005
HCl extractable Fe ³⁺ (mmol kg ⁻¹)	Control	0.719	0.004	0.868	0.009
	Biochar	0.782	0.008	0.934	0.010
H ₂ O extractable total P (mg P kg ⁻¹)	Control	1.315	0.282	0.795	0.059
	Biochar	1.045	0.157	1.195	0.111
Solid total P (mg P kg ⁻¹)	Control	932	33	926	44
	Biochar	904	46	867	33

78

79 *Table S8: Time sequence of belowground C allocation to Soil + Root respiration and root biomass in control and field-aged biochar-amended soils at 8.9- (a),*
 80 *9.2- (b) and 9.5- (c) month pulse labelling event (n=3). Standard errors are presented.*

(a)		Control							
Days after 8.9-year labelling	3		5		10		15		
C allocation (g ¹³ C m ⁻²)	Mean	SE	Mean	SE	Mean	SE	Mean	SE	
Soil + Root respiration	1.22E-04	8.47E-05	4.82E-04	6.28E-05	8.99E-04	2.53E-04	5.47E-03	8.09E-04	
Root biomass	0.0951	0.00912	0.0826	0.00754	0.0507	0.00727	0.0549	0.00351	
		Field-aged biochar							
Days after 8.9-year labelling	3		5		10		15		
C allocation (g ¹³ C m ⁻²)	Mean	SE	Mean	SE	Mean	SE	Mean	SE	
Soil + Root respiration	2.02E-04	1.01E-05	1.45E-04	1.29E-05	1.70E-03	5.91E-04	7.88E-03	1.47E-03	
Root biomass	0.0993	0.01231	0.0889	0.00592	0.0511	0.00684	0.0542	0.00300	

81

(b)		Control							
Days after 9.2-year labelling	3		5		10		15		
C allocation (g ¹³ C m ⁻²)	Mean	SE	Mean	SE	Mean	SE	Mean	SE	
Soil + Root respiration	1.72E-04	9.39E-05	5.97E-04	4.22E-05	6.59E-04	2.96E-04	2.58E-04	1.65E-04	
Root biomass	0.0819	0.0133	0.0737	0.00670	0.0507	0.01388	0.0411	0.00285	
		Field-aged biochar							
Days after 9.2-year labelling	3		5		10		15		
C allocation (g ¹³ C m ⁻²)	Mean	SE	Mean	SE	Mean	SE	Mean	SE	
Soil + Root respiration	1.13E-04	1.03E-05	1.72E-03	3.72E-04	1.05E-03	5.08E-04	4.37E-04	1.55E-04	
Root biomass	0.0896	0.00891	0.0780	0.00508	0.0331	0.000519	0.0411	0.00311	

82

(c)	Control							
	3		5		10		15	
Days after 9.5-year labelling	Mean	SE	Mean	SE	Mean	SE	Mean	SE
C allocation (g ¹³ C m ⁻²)								
Soil + Root respiration	7.61E-04	2.20E-05	1.76E-04	5.73E-05	1.39E-03	1.04E-04	1.08E-03	3.19E-04
Root biomass	0.0882	0.00724	0.0792	0.00512	0.0573	0.00115	0.0187	0.00230
	Field-aged biochar							
Days after 9.5-year labelling	3		5		10		15	
C allocation (g ¹³ C m ⁻²)	Mean	SE	Mean	SE	Mean	SE	Mean	SE
Soil + Root respiration	4.88E-04	2.03E-04	1.42E-04	8.21E-05	2.14E-03	9.20E-04	1.43E-03	1.12E-04
Root biomass	0.0945	0.04925	0.0802	0.00235	0.0493	0.00125	0.0343	0.00251

83

84 *Table S9: Belowground C allocation to bulk soil and soil fractions in control and field-aged biochar-amended soils on Day 15 of 8.9-, 9.2- and 9.5-year pulse*
85 *labelling event (n=3). Standard errors are presented.*

	Day 15 of 8.9-year labelling				Day 15 of 9.2-year labelling				Day 15 of 9.5-year labelling			
	Control		Field-aged biochar		Control		Field-aged biochar		Control		Field-aged biochar	
C allocation (g ¹³ C m ⁻²)	Mean	SE	Mean	SE	Mean	SE	Mean	SE	Mean	SE	Mean	SE
Bulk soil	0.0169	0.0031	0.0226	0.0172	0.0344	0.0202	0.0417	0.0096	0.0590	0.0103	0.0739	0.0190
Free POM (250-2000 μm)	0.00058	0.00112	0.00062	0.00117	0.00143	0.00115	0.00120	0.00086	0.00417	0.00299	0.00261	0.00246
Free POM (<250 μm)	0.00070	0.00127	0.00063	0.00092	0.00156	0.00154	0.00105	0.00094	0.00372	0.00271	0.00260	0.00190
Occluded POM (250-2000 μm)	0.00538	0.00192	0.00860	0.00230	0.00597	0.00038	0.00627	0.00276	0.00793	0.00166	0.01117	0.00498
Occluded POM (<250 μm)	0.00202	0.00211	0.00362	0.00104	0.00657	0.00055	0.00560	0.00064	0.00855	0.00088	0.01246	0.00354
Mineral SOM (250-2000 μm)	0.00427	0.00218	0.00476	0.00264	0.01039	0.00014	0.01302	0.00241	0.01808	0.00025	0.02133	0.00128
Mineral SOM (<250 μm)	0.00331	0.00082	0.00382	0.00109	0.00656	0.00234	0.01223	0.00072	0.01141	0.00030	0.02003	0.00075

86

87 *Table S10. XPS of the C functional groups measured on a finely crushed <250 μm microaggregate*
 88 *fraction, with and without biochar, and the crushed 250-2000 μm microaggregate fraction, with and*
 89 *without biochar. Note that other functional groups (such as N and O etc.) are omitted here.*

Name	Functional Groups	9.5 year	Unamended	9.5 year	Unamended
		biochar-	control	biochar-	control
		amended		amended	
		250-2000	250-2000	<250 μm	<250 μm
		μm	μm		
		Atomic %	Atomic %	Atomic %	Atomic %
C1s A	C-C/C-H/C=C	8.59	8.67	9.46	9.25
C1s B	C-O/C-O-C/C-N	6.85	7.03	8.07	7.11
C1s C	C=O	2.46	2.3	2.77	2.52
C1s D	COOH	2.17	2.04	2.47	1.94

90

91 *Table S11: Aboveground biomass within the control and field-aged biochar-amended soils harvested*
 92 *7 days before 8.9-, 9.2- and 9.5-year pulse labelling event. Note that this ryegrass is a winter breed.*
 93 *Ryegrass was not active during the summer at 9.2-year time. Standard errors are given (n=3).*

	8.9-year time		9.2-year time		9.5-year time	
	Yield (g dry wt. m ⁻²)	SE	Yield (g dry wt. m ⁻²)	SE	Yield (g dry wt. m ⁻²)	SE
Control	293	17.4	230	10.4	429	10.6
Biochar	349	23.1	276	31.3	442	5.6

94